Steroids 171 (2021) 108830

Contents lists available at ScienceDirect

Steroids

journal homepage: www.elsevier.com/locate/steroids

Synthesis and anti-inflammatory activity of novel steroidal chalcones with 3β-pregnenolone ester derivatives in RAW 264.7 cells *in vitro*

Xiaorui Cai [a,1], Fei Sha [a,1], Chuanyi Zhao [b], Zhiwei Zheng [a], Shulin Zhao [a], Zhiwei Zhu [a], Huide Zhu [a], Jiaoling Chen [a], Yicun Chen [b,*]

[a] Department of Pharmacy, The Affiliated Tumor Hospital of Shantou University Medical College, Shantou 515041, Guangdong, China
[b] Department of Pharmacology, Shantou University Medical College, Shantou 515041, Guangdong, China

ARTICLE INFO

Keywords:
Steroid
Pregnenolone
Chalcones
Cinnamic acid derivatives
Anti-inflammatory activity
RAW 264.7 cells

ABSTRACT

To identify new potential anti-inflammatory agents, we herein report the synthesis of novel steroidal chalcones with 3β-pregnenolone esters of cinnamic acid derivatives using pregnenolone as the starting material. The structures of the newly synthesised compounds were confirmed by ^{1}H NMR, ^{13}C NMR, HRMS and infrared imaging. All the derivatives were examined to determine their *in vitro* anti-inflammatory profiles against LPS-induced inflammation in RAW 264.7 cells; the derivates were evaluated by the quantification of the pro-inflammatory mediator nitric oxide (NO) in the cell culture supernatant based on the Griess reaction, which measures nitrite levels, followed by an *in vitro* cytotoxicity study. Among these novel derivatives, compound **11e** [3β-3-phenyl acrylate-pregn-5-en-17β-yl-3′ -(p-fluoro)-phenylprop-2′-en-1′-one] was identified as the most potent anti-inflammatory agent, which showed significant anti-inflammatory activity by inhibiting the LPS-induced pro-inflammatory mediator NO in a dose-dependent manner without any cytotoxicity. Moreover, compound **11e** markedly inhibited the expression of pro-inflammatory cytokines, including inducible nitric oxide synthase (iNOS), interleukin-6 (IL-6), tumour necrosis factor-α (TNF-α), and cyclooxygenase-2 (COX-2), in LPS-induced RAW 264.7 cells. Further studies confirmed that compound **11e** significantly suppressed the transcriptional activity of NF-κB in activated RAW 264.7 cells. Molecular docking study revealed the strong binding affinity of compound **11e** to the active site of the pro-inflammatory proteins, which confirmed that compound **11e** acted as an anti-inflammatory mediator. These results indicated that steroidal chalcones with 3β-pregnenolone esters of cinnamic acid derivatives might be considered for further research in the design of anti-inflammatory drugs, and compound **11e** might be a promising therapeutic anti-inflammatory drug candidate.

1. Introduction

Inflammation is the body's self-defence system that protects organisms from harmful stimuli, and it is characterized by pain, heat, swelling, redness, and loss of function of the affected body part [1]. When inflammatory reactions are exaggerated or inadequate, they can lead to physiological decompensation, organ dysfunction, and even death [2,3].

The inflammatory responses of organisms are triggered by various stimuli, including physical, chemical and biological stimuli, resulting in the recruitment of inflammatory and innate immune cells to the site of injury or infection. In response to extracellular stimuli, macrophages can produce and release pro-inflammatory mediators, such as NO, prostaglandin E2 (PGE-2), interleukin-1 beta (IL-1β), TNF-α and other inflammatory mediators [4,5]. However, severe or chronic inflammation is highly related to diseases, such as osteoarthritis, rheumatoid arthritis and diabetes, because of the increased production of pro-inflammatory mediators [6,7]. Therefore, macrophages may be a potential therapeutic target for inflammatory diseases.

However, the chronic use of anti-inflammatory drugs is limited due to their severe side effects, such as gastrointestinal injury, especially gastrointestinal perforation, peptic ulceration or significant bleeding. Thus, the development of new therapeutic agents that can avoid gastrointestinal injury and lead to enhanced anti-inflammatory effects has become an urgent need for patients with inflammatory diseases [8,9].

Lipopolysaccharide (LPS) is a component of the outer membrane of

* Corresponding author.
E-mail address: chenyicun@yeah.net (Y. Chen).
[1] Xiaorui Cai and Fei Sha contributed equally to this article.

https://doi.org/10.1016/j.steroids.2021.108830
Received 14 January 2021; Received in revised form 5 March 2021; Accepted 28 March 2021
Available online 6 April 2021

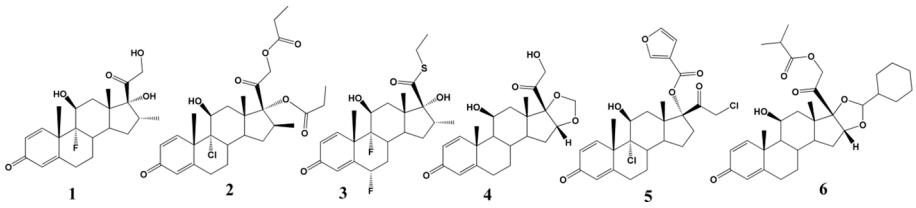

Fig. 1. Structures of standard anti-inflammatory steroid drugs; dexamethasone (1), beclometasone dipropionate (2), fluticasone (3), budesonide (4), mometasone (5) and ciclesonide (6).

Gram-negative bacteria and a potent inducer of the differentiation of monocytes to M1-like, classically activated macrophages, which produce pro-inflammatory mediators, such as NO, PGE-2, iNOS, COX-2, TNF-α, IL-6 and IL-1β [10,11]. Furthermore, LPS is known to activate the nuclear factor-kappa B (NF-κB) and mitogen-activated protein kinase (MAPK) signalling pathways through the activation of Toll-like receptors (TLRs) [12,13].

MAPKs are known as upstream molecules of the NF-κB signalling pathway that play a pivotal role in governing the inflammatory process and are activated by LPS [14,15]. Consisting of three well-defined parallel modules, p38, extracellular signal-regulated kinase (ERK), and c-Jun *N*-terminal kinase (JNK), MAPKs are implicated in the regulation of COX-2 and iNOS expression [16]. MAPK activation contributes to the activation of transcription factors such as NF-κB, which is largely implicated in the expression of anti-inflammatory mediators, including NO, PGE-2, IL-6, IL-1β, and TNF-α [17].

Steroidal compounds exhibit a variety of biological functions, play a very important role in biology [18] and have attracted profound attention in the development of potent pharmacological agents for the treatment of various diseases, including cardiovascular disease, autoimmune disorders, adrenal insufficiencies, and fungal and microbial infections. Steroids are a very important class of anti-inflammatory agents (SAIAs). Steroids suppress the immune response through the inhibition of NF-κB and the suppression of pro-inflammatory cytokines. Steroids also inhibit the production of prostaglandins and leukotrienes. Some of the notable steroidal anti-inflammatory drugs are dexamethasone (1), beclometasone dipropionate (2), fluticasone (3), budesonide (4), mometasone (5), and ciclesonide (6) (Fig. 1). These drugs are used for the management of various human disease conditions associated with inflammation [19,20]. Steroid-based chemotherapeutic drugs possess various advantages, such as low toxicity, low vulnerability to multidrug resistance (MDR) and high bioavailability, because they are capable of penetrating the cell wall [21].

Chalcones (1, 3-diphenyl-2-propen-1-one) are well known for their diverse array of bioactivities. In particular, chalcones have been reported to possess pharmacological activities, such as anticancer, antioxidant, anti-inflammatory [22,23], and antimicrobial activities [24,25]. The chalcone structure consists of three important components, viz. two phenyl rings and an a,b-unsaturated carbonyl system that joins them. Previous studies have revealed that the nature of the substituents on the phenyl rings and their conformation in the core structure play a vital role in determining their activities. In some specific studies, it was found that variations leading to conformational changes, such as epoxidation or substitution on the double bond, result in decreased bioactivity [26].

Pregnenolone is a naturally occurring neurosteroid that is synthesized from cholesterol in the adrenal gland and the central nervous system and is known as a precursor to other hormones, including cortisone, oestrogen, testosterone and progesterone [27,28]. Pregnenolone is an active ingredient in many traditional Chinese medicines that possess good anti-inflammatory activity, such as *Rhizoma ligustici wallichii*, which shows strong anti-inflammatory and analgesic effects [29].

Cinnamic acid is one of the main chemical ingredients in *Cinnamomum cassia*. It has been reported that cinnamic acid and its analogue, styryl ketone, possess good antioxidative and anti-inflammatory properties [30–32].

The coupling of two or more natural products to make hybrids leads to an almost inexhaustible reservoir of new types of compounds with diverse structures [25]. The underlying expectation is that a combination of structural features of two or more functionally active substances into one molecule or their covalent coupling may either enhance or modulate the desired characteristics of the individual components or lead to new types of properties [33,34]. Previous literatures have been reported that such structure like steroidal chalcones have been shown to bear a lot of different biological activities such as antimicrobial, anti-inflammatory, anticancer, antioxidant, and hypotensive activities [35–38].

In this study, we prepared a novel class of modified steroids or chalcone analogues or chalconoyl pregnenolones with 3β-pregnenolone esters of cinnamic acid using pregnenolone as the steroid precursor. The 17-acetyl group of pregnenolone was used to form the enol using the Claisen–Schmidt condensation method to condense different aromatic aldehydes to synthesize a series of chalconoyl pregnenolones. In a later step, we successfully applied Steglich esterification to produce a novel class of steroidal chalcones with 3β-pregnenolone ester derivatives using cinnamic acid. The anti-inflammatory capacities of these synthetic compounds and their underlying mechanisms were assessed in RAW 264.7 macrophage cells. The results show that compound **11e** exhibited the most potent anti-inflammatory properties among the members of this family. Compound **11e** showed the most potent activity in the inhibition of NO production, significantly inhibited the expression of pro-inflammatory factors, such as IL-6, TNF-α and PGE-2, and suppressed the transcriptional activity of NF-κB signalling in LPS-induced RAW 264.7 cells.

2. Materials and methods

2.1. Chemistry

2.1.1. Reagent and instrument

All reagents were purchased from commercial suppliers. Melting points were determined using an Electrothermal 9100 melting point apparatus (Weiss-Gallenkamp, Loughborough, UK). Thin-layer chromatography (TLC) was performed on silica gel F254 plates and visualized by UV light or iodine vapour. IR spectra were recorded on an Is5 FT-IR spectrophotometer (Nicolet, Thermo, Waltham, MA, USA) as KBr pellets or thin films. ^{1}H NMR spectra of $CDCl_3$ solutions (tetramethylsilane as an internal standard) were recorded on an AVANCE II-600 (600 MHz) spectrometer (Bruker, Karlsruhe, Germany). Mass spectra were recorded on a SCIEX Triple Quad 6500 + LC/MS/MS system (SCIEX, Los Angeles, CA, USA). HRMS (high-resolution mass spectrometry) was performed on a Q-FT-MS system (SolariX 7 T, Bruker, USA). ^{13}C NMR spectra were measured at 150 MHz on a Bruker AVANCE III spectrometer. Chalcones were prepared from substituted benzaldehyde and pregnenolone according to the procedure reported in the literature.

2.1.2. Chemical methods

*2.1.2.1. General synthesis of 3β-hydroxy-pregn-5-en-17β-yl-3′-phenylprop-2′-en-1′-one derivatives (**9a–9i**).* To a solution of pregnenolone **7** (3.16 g, 0.01 mol) in ethanol (30 mL), a conc. Aq. Solution of NaOH (1.0 g, 0.025 mol) was added. Then, aldehyde **8** (0.012 mol) was added to the reaction mixture and stirred at room temperature for 48 h to obtain the corresponding benzylidine derivative **9 (9a–9i)**. The progress of the reaction was monitored by TLC (petroleum ether: ethyl acetate (2:1 v/v) as eluents). After completion, the reaction mixture was poured into crushed ice water. The precipitate was filtered, dried and recrystallized from ethanol to yield the product as a solid white powder [39,40]. It should be mentioned that when non-aromatic aldehydes were used, the product was formed in a very minor quantity and was not sufficiently stable under ambient conditions. Thus, the study was restricted to the use of only aromatic aldehydes, for which the obtained yields were 75–86%.

*2.1.2.1.1. 3β-hydroxy-pregn-5-en-17β-yl-3′-(p-benzyloxy)-phenylprop-2′-en-1′-one **(9a)**.*. White solid powder (Yield, 82.40%), M.p.: 218.4–219.4 °C. ^{1}H NMR (400 MHz, δ ppm, $CDCl_3$): 7.47–7.57 (m, 3H, C = CH , Ar-H), 7.32–7.44 (m, 5H, Ar-H), 6.98 (d, 2H, *J* = 8.4 Hz, Ar-H), 6.65 (d, 1H, *J* = 16.0 Hz, CH = C), 5.37 (s, 1H, C_6-H), 5.10 (s, 2H), 3.51–3.56 (m, 1H, C_3α-H), 2.83 (m, 1H, C_{17}α-H), 1.00 (s, 3H, C_{10}-CH_3), 0.63 (s, 3H, C_{13}-CH_3). ^{13}C NMR (ppm, $CDCl_3$): 200.34, 160.62, 141.46, 140.83, 136.47, 129.99(2C), 128.67(2C), 128.16, 127.45(3C), 124.82, 121.41, 115.30(2C), 71.68, 70.12, 61.99, 57.20, 50.12, 44.96, 42.26, 39.15, 37.29, 36.56, 32.04, 31.88, 31.61, 24.71, 22.81, 21.14, 19.40, 13.42. MS (ESI) (*m/z*):511.3 $[M + H]^+$.

*2.1.2.1.2. 3β-hydroxy-pregn-5-en-17β-yl-3′-(p-methoxy)-phenylprop-2′-en-1′-one **(9b)**.*. Yellow solid (Yield: 85.16%), M.p.: 102.8–105.8 °C. ^{1}H NMR (400 MHz, δ ppm, $CDCl_3$): 7.48–7.56 (m, 3H, C = CH , Ar-H), 6.93 (d, 2H, *J* = 8.4 Hz, Ar-H), 6.66 (d, 1H, *J* = 16.0 Hz, CH = C), 5.39 (s, 1H, C_6-H), 3.87 (s, 3H, $C_{4''}$–OCH_3), 3.53–3.56 (m, 1H, C_3α-H), 2.86 (m, 1H, C_{17}α-H), 1.02 (s, 3H, C_{10}-CH_3), 0.66 (s, 3H, C_{13}-CH_3). ^{13}C NMR (ppm, $CDCl_3$): 200.35, 161.45, 141.33, 140.84, 129.97(3C), 124.70, 121.37, 114.39(2C), 71.64, 61.95, 57.18, 55.39, 50.11, 44.95, 42.24, 39.12, 37.28, 36.54, 32.02, 31.86, 31.58, 24.70, 22.81, 21.13, 19.38, 13.40. MS (ESI) (*m/z*): 435.3 $[M + H]^+$.

*2.1.2.1.3. 3β-hydroxy-pregn-5-en-17β-yl-3′-(p-bromo)-phenylprop-2′-en-1′-one **(9c)**.*. White solid powder (Yield, 77.89%), M.p.: 144.8–145.6 °C. ^{1}H NMR (400 MHz, δ ppm, $CDCl_3$): 7.42–7.55 (m, 5H, C = CH , Ar-H), 6.67 (d, 1H, *J* = 16.0 Hz, CH = C), 5.39 (s, 1H, C_6-H), 3.50–3.56 (m, 1H, C_3α-H), 2.83 (m, 1H, C_{17}α-H), 1.02 (s, 3H, C_{10}-CH_3), 0.65 (s, 3H, C_{13}-CH_3). ^{13}C NMR (ppm, $CDCl_3$): 200.17, 140.79, 140.08, 133.77, 132.14(2C), 129.63(2C), 127.25, 124.48, 121.39, 71.69, 62.25, 57.19, 50.08, 45.05, 42.25, 39.16, 37.27, 36.54, 32.02, 31.84, 31.61, 24.67, 22.76, 21.12, 19.38, 13.45. MS (ESI) (*m/z*): 483.2, 485.2 $[M + H]^+$.

*2.1.2.1.4. 3β-hydroxy-pregn-5-en-17β-yl-3′-(p- chloro)-phenylprop-2′-en-1′-one **(9d)**.* Light yellow solid (Yield: 81.48%), M.p.: 148.5–151.4 °C. ^{1}H NMR (400 MHz, δ ppm, $CDCl_3$): 7.41–7.53 (m, 3H, C = CH , Ar-H), 7.36 (d, *J* = 8.0 Hz, 2H, Ar-H), 6.74 (d, 1H, *J* = 16.0 Hz, CH = C), 5.36 (s, 1H, C_6-H), 3.50–3.54 (m, 1H, C_3α-H), 2.84 (m, 1H, C_{17}α-H), 1.00 (s, 3H, C_{10}-CH_3), 0.64 (s, 3H, C_{13}-CH_3). ^{13}C NMR (ppm, $CDCl_3$): 200.16, 140.79, 140.02, 136.15, 133.34, 129.41(2C), 129.18 (2C), 127.16, 121.39, 71.69, 62.24, 57.19, 50.08, 45.04, 42.25, 39.17, 37.27, 36.54, 32.02, 31.84, 31.61, 24.67, 22.76, 21.12, 19.38, 13.45. MS (ESI) (*m/z*): 439.3 $[M + H]^+$.

*2.1.2.1.5. 3β-hydroxy-pregn-5-en-17β-yl-3′-(p-fluoro)-phenylprop-2′-en-1′-one **(9e)**.*. White solid powder (Yield, 75.02%), M.p.: 105.6–108.1 °C. ^{1}H NMR (400 MHz, δ ppm, $CDCl_3$): 7.43–7.56 (m, 3H, C = CH , Ar-H), 6.89 (d, 2H, *J* = 8.0 Hz, Ar-H), 6.66 (d, 1H, *J* = 16.0 Hz, CH = C), 5.36 (s, 1H, C_6-H), 3.48–3.54 (m, 1H, C_3α-H), 2.84 (m, 1H, C_{17}α-H), 1.00 (s, 3H, C_{10}-CH_3), 0.63 (s, 3H, C_{13}-CH_3). ^{13}C NMR (ppm, $CDCl_3$): 200.34, 160.86, 141.40, 140.81, 130.13, 129.97(2C), 127.31, 121.40, 114.87(2C), 71.67, 63.63, 61.95, 57.19, 50.12, 44.94, 42.25, 39.13, 37.28, 36.54, 32.02, 31.86, 31.59, 24.70, 22.81, 21.13, 19.38, 14.71, 13.40. MS (ESI) (*m/z*): 423.3 $[M + H]^+$.

*2.1.2.1.6. 3β-hydroxy-pregn-5-en-17β-yl-3′-(p-tolyl)-phenylprop-2′-en-1′-one **(9f)**.*. Light yellow solid (Yield: 85.36%), M.p.: 123.5–126.4 °C. ^{1}H NMR (400 MHz, δ ppm, $CDCl_3$): 7.53 (d, 1H, *J* = 16.0 Hz, C = CH),7.46 (d, 2H, *J* = 8.0, Ar-H), 7.20 (d, 2H, *J* = 8.0 Hz, Ar-H), 6.74 (d, 1H, *J* = 16.0 Hz, CH = C), 5.36 (s, 1H, C_6-H), 3.51–3.54 (m, 1H, C_3α-H), 2.85 (m, 1H, C_{17}α-H), 2.38 (s, 3H, $C_{4''}$–CH_3), 1.00 (s, 3H, C_{10}-CH_3), 0.64 (s, 3H, C_{13}-CH_3). ^{13}C NMR (ppm, $CDCl_3$): 200.45, 141.58, 140.75, 132.07, 129.65(2C), 128.29(2C), 127.13, 125.94, 121.42, 71.70, 61.98, 57.21, 50.11, 44.97, 42.26, 39.14, 37.28, 36.55, 32.03, 31.86, 31.61, 24.70, 22.79, 21.48, 21.13, 19.38, 13.42. MS (ESI) (*m/z*): 419.3 $[M + H]^+$.

*2.1.2.1.7. 3β-hydroxy-pregn-5-en-17β-yl-3′-(m,p-dimethoxy)-phenylprop-2′-en-1′-one **(9 g)**.*. Yellow solid powder (Yield, 83.27%), M.p.:100.4–101.4 °C. ^{1}H NMR (400 MHz, δ ppm, $CDCl_3$): 7.52 (d, 1H, *J* = 16.0 Hz, C = CH),7.14–7.18 (m, 1H, Ar-H), 7.06–7.10 (m, 1H, Ar-H), 6.89 (d, 1H, *J* = 8.0 Hz, Ar-H), 6.67 (d, 1H, *J* = 16.0 Hz, CH = C), 5.38 (s, 1H, C_6-H), 3.94 (s, 6H, $C_{3'',\ 4''}$–OCH_3), 3.51–3.56 (m, 1H, C_3α-H), 2.89 (m, 1H, C_{17}α-H), 1.01 (s, 3H, C_{10}-CH_3), 0.64 (s, 3H, C_{13}-CH_3). ^{13}C NMR (ppm, $CDCl_3$): 200.32, 151.22, 149.24, 141.66, 140.82, 127.76, 125.04, 122.73, 121.37, 111.17, 110.14, 71.64, 61.69, 57.21, 55.98 (2C), 50.12, 44.97, 42.23, 39.09, 37.29, 36.54, 32.02, 31.86, 31.57, 24.70, 22.90, 21.13, 19.38, 13.42. MS (ESI) (*m/z*): 465.4 $[M + H]^+$.

*2.1.2.1.8. 3β-hydroxy-pregn-5-en-17β-yl-3′-(p-methylthio)-phenylprop-2′-en-1′-one **(9 h)**.*. Yellow solid powder (Yield, 80.16%), M.p.:155.2–156.4 °C. ^{1}H NMR (400 MHz, δ ppm, $CDCl_3$): 7.44–7.60 (m, 3H, C = CH , Ar-H), 7.25 (d, 2H, *J* = 8.0 Hz, Ar-H), 6.76 (d, 1H, *J* = 16.0 Hz, CH = C), 5.39 (s, 1H, C_6-H), 3.53–3.56 (m, 1H, C_3α-H), 2.86 (m, 1H, C_{17}α-H), 2.53 (s, 3H, $C_{4''}$-SCH_3),1.02 (s, 3H, C_{10}-CH_3), 0.66 (s, 3H, C_{13}-CH_3). ^{13}C NMR (ppm, $CDCl_3$): 200.30, 141.95, 140.95, 131.35, 128.63 (3C), 126.07(2C), 125.86, 121.41, 71.70, 62.08, 57.20, 50.10, 45.00, 42.26, 39.14, 37.27, 36.54, 32.03, 31.86, 31.61, 24.69, 22.79, 21.13, 19.38, 15.21, 13.43. MS (ESI) (*m/z*): 451.3 $[M + H]^+$.

*2.1.2.1.9. 3β-hydroxy-pregn-5-en-17β-yl-3′-(o-fluoro)-phenylprop-2′-en-1′-one **(9i)**.*. White solid powder (Yield, 85.19%), M.p.: 140.6–142.2 °C. ^{1}H NMR (400 MHz, δ ppm, $CDCl_3$): 7.67 (d, 1H, *J* = 16.0 Hz, C = CH),7.55–7.58 (m, 1H, Ar-H), 7.34–7.39 (m, 1H, Ar-H), 7.08–7.19 (m, 2H, Ar-H), 6.88 (d, 1H, *J* = 16.0 Hz, CH = C), 5.37 (s, 1H, C_6-H), 3.48–3.60 (m, 1H, C_3α-H), 2.88 (m, 1H, C_{17}α-H), 1.00 (s, 3H, C_{10}-CH_3), 0.64 (s, 3H, C_{13}-CH_3). ^{13}C NMR (ppm, $CDCl_3$): 200.50, 162.48, 160.80, 140.80, 134.15, 131.60, 129.32, 124.45, 122.93, 121.40, 116.20, 71.69, 61.97, 57.19, 50.06, 44.99, 42.25, 39.07, 37.27, 36.54, 32.03, 31.85, 31.61, 24.68, 22.78, 21.14, 19.38, 13.47. MS (ESI) (*m/z*): 423.3 $[M + H]^+$.

*2.1.2.2. General synthesis of 3β-3-phenyl acrylates-pregn-5-en-17β-yl-3′-phenylprop-2′-en-1′-one derivatives **(11a-11i)**.* A suspension of compounds **9a-9i** (0.01 mol), cinnamic acid **10** (2.96 g, 0.02 mol), EDCI (0.38 g, 2 mmol) and DMAP (0.12 g, 1 mmol) in dry dichloromethane (25 mL) was stirred at room temperature for 48 h and filtered. The filtrate was washed with 5% $NaHCO_3$ liquor (3 × 15 mL), dried over $MgSO_4$, filtered, and concentrated in vacuo. The residue was purified by silica gel column chromatography (petroleum ether/ethyl acetate, 5:1) to afford the corresponding ester [41]. Quantitative yields of 51–75% were obtained for compounds **11a–11i**.

*2.1.2.2.1. 3β-3-phenyl acrylates-pregn-5-en-17β-yl-3′-(p-benzyloxy)-phenylprop-2′-en-1′-one **(11a)**.* White solid powder (Yield, 68.22%), M.p.: 175.0–178.0 °C. IR (KBr, cm^{-1}): 1704.94 (C═O), 1676.32, 1644.07, 1597.91, 1573.72, 1510.07, 1452.17, 1174.75 (C—O), 1097.02 (C—O). ^{1}H NMR (600 MHz, δ ppm, $CDCl_3$): 7.68 (d, 1H, *J* = 16.20 Hz, C = CH), 7.50–7.53 (m, 5H, C = CH, Ar-H), 7.33–7.46 (m, 8H, Ar-H), 6.98 (d, 2H, *J* = 9.0 Hz, Ar-H), 6.67 (d, 1H, *J* = 15.60 Hz, CH = C), 6.43 (d, 1H, *J* = 16.20 Hz, CH = C), 5.42 (s, 1H, C_6-H), 5.11 (s, 2H), 4.73–4.79 (m, 1H, C_3α-H), 2.85 (m, 1H, C_{17}α-H), 1.04 (s, 3H, C_{10}-CH_3), 0.65 (s, 3H, C_{13}-

CH_3). ^{13}C NMR (ppm, $CDCl_3$): 200.25, 166.41, 160.60, 144.48, 141.20, 139.72, 136.47, 134.53, 130.19, 129.98(2C), 128.87(2C), 128.68(2C), 128.16, 128.04(3C), 127.76, 127.45(2C), 124.86, 122.47, 118.68, 115.28(2C), 73.98, 70.11, 61.96, 57.15, 50.04, 44.94, 39.12, 38.21, 37.06, 36.68, 32.01, 31.89, 27.88, 24.71, 22.80, 21.10, 19.35, 13.42. MS (ESI) (*m/z*): 641.3 $[M + H]^+$. HRMS (EI): *m/z* $[M + Na]^+$ calcd for $C_{44}H_{48}O_4$: 663.3450; found: 663.344385.

2.1.2.2.2. 3β-3-phenyl acrylates -pregn-5-en-17β-yl-3′-(p-methoxy)-phenylprop-2′-en-1′-one ***(11b)***. Yellow solid powder (Yield: 51.23%), M.p.: 164.4–167.3 °C. IR (KBr, cm^{-1}): 1700.18 (C═O), 1677.34, 1644.76, 1597.74, 1573.53, 1510.91, 1451.52, 1172.76 (C—O), 1098.08 (C—O). ^1H NMR (600 MHz, δ ppm, $CDCl_3$): 7.68 (d, 1H, *J* = 16.20 Hz, C = CH), 7.51–7.56 (m, 5H, C = CH, Ar-H), 7.33–7.41 (m, 3H, Ar-H), 6.91 (d, 2H, *J* = 8.40 Hz, Ar-H), 6.67 (d, 1H, *J* = 16.20 Hz, CH = C), 6.43 (d, 1H, *J* = 16.20 Hz, CH = C), 5.42 (s, 1H, C_6-H), 4.72–4.79 (m, 1H, C_3α-H), 3.84 (s, 3H, $C_{4''}$–OCH_3), 2.85 (m, 1H, C_{17}α-H), 1.04 (s, 3H, C_{10}-CH_3), 0.65 (s, 3H, C_{13}-CH_3). ^{13}C NMR (ppm, $CDCl_3$): 200.25, 166.4, 161.46, 144.47, 141.27, 139.72, 134.53, 130.19, 129.97(3C), 128.87(2C), 128.04(2C), 127.52, 124.76, 122.47, 118.68, 114.39(2C), 73.98, 61.93, 57.14, 55.40, 50.04, 44.93, 39.10, 38.21, 37.06, 36.68, 32.12, 31.95, 27.88, 24.71, 22.81, 21.05, 19.33, 13.41. MS (ESI) (*m/z*): 565.3 $[M + H]^+$. HRMS (EI): *m/z* $[M + Na]^+$ calcd for $C_{38}H_{44}O_4$: 587.3137; found: 587.313051.

2.1.2.2.3. 3β-3-phenyl acrylates -pregn-5-en-17β-yl-3′-(p-bromo)-phenylprop-2′-en-1′-one ***(11c)***. Light yellow solid powder (Yield: 52.67%), M.p.: 169.3–172.6 °C. IR (KBr, cm-1): 1708.13 (C═O), 1678.78, 1644.75, 1603.46, 1562.25, 1486.96, 1450.74, 1175.02 (C—O), 1096.08 (C—O). ^1H NMR (600 MHz, δ ppm, $CDCl_3$): 7.68 (d, 1H, *J* = 15.60 Hz, C = CH), 7.46–7.52 (m, 5H, C = CH, Ar-H), 7.33–7.44 (m, 5H, Ar-H), 6.76 (d, 1H, *J* = 15.60 Hz, CH = C), 6.43 (d, 1H, *J* = 16.20 Hz, CH = C), 5.41 (s, 1H, C_6-H), 4.75–4.81 (m, 1H, C_3α-H), 2.84 (m, 1H, C_{17}α-H), 1.04 (s, 3H, C_{10}-CH_3), 0.64 (s, 3H, C_{13}-CH_3). ^{13}C NMR (ppm, $CDCl_3$): 200.09, 166.39, 144.49, 140.06, 139.71, 134.52, 133.78, 132.16(2C), 130.20, 129.65(2C), 128.88(4C), 128.04(2C), 127.28, 124.49, 122.42, 118.67, 73.95, 62.21, 57.13, 50.00, 45.03, 39.13, 38.21, 37.06, 36.66, 32.10, 31.93, 27.88, 24.68, 22.77, 21.09, 19.35, 13.47. MS (ESI) (*m/z*): 613.2, 615.3 $[M + H]^+$. HRMS (EI): *m/z* $[M + Na]^+$ calcd for $C_{37}H_{41}BrO_3$: 635.2137; found: 635.213063.

2.1.2.2.4. 3β-3-phenyl acrylates -pregn-5-en-17β-yl-3′-(p-chloro)-phenylprop-2′-en-1′-one ***(11d)***. Light yellow solid powder (Yield: 58.10%), M.p.: 182.0–182.6 °C. IR (KBr, cm^{-1}): 1709.47 (C═O), 1679.60, 1644.94, 1604.24, 1566.52, 1490.85, 1451.19, 1175.80 (C—O), 1091.46 (C—O). ^1H NMR (600 MHz, δ ppm, $CDCl_3$): 7.68 (d, 1H, *J* = 16.20 Hz, C = CH), 7.46–7.57 (m, 5H, C = CH, Ar-H), 7.33–7.43 (m, 5H, Ar-H), 6.75 (d, 1H, *J* = 15.60 Hz, CH = C), 6.43 (d, 1H, *J* = 15.60 Hz, CH = C), 5.42 (s, 1H, C_6-H), 4.73–4.78 (m, 1H, C_3α-H), 2.85 (m, 1H, C_{17}α-H), 1.04 (s, 3H, C_{10}-CH_3), 0.65 (s, 3H, C_{13}-CH_3). ^{13}C NMR (ppm, $CDCl_3$): 200.10, 166.40, 144.49, 140.00, 139.55, 136.15, 134.52, 133.35, 130.20, 129.43(2C), 129.19(2C), 128.88(2C), 128.04(2C), 127.20, 122.42, 118.66, 73.95, 62.20, 57.13, 50.01, 45.03, 39.13, 38.20, 37.06, 36.67, 32.12, 31.90, 27.88, 24.68, 22.77, 21.09, 19.35, 13.47. MS (ESI) (*m/z*): 569.2, 570.2 $[M + H]^+$. HRMS (EI): *m/z* $[M + Na]^+$ calcd for $C_{37}H_{41}ClO_3$: 591.2642; found: 591.263562.

2.1.2.2.5. 3β-3-phenyl acrylates -pregn-5-en-17β-yl-3′-(p-fluoro)-phenylprop-2′-en-1′-one ***(11e)***. Yellow solid powder (Yield: 66.57%), M.p.: 174.8–177.2 °C. IR (KBr, cm^{-1}): 1703.61 (C═O), 1677.03, 1643.59, 1597.65, 1573.65, 1510.26, 1451.13, 1173.80 (C—O), 1097.14(C—O). ^1H NMR (600 MHz, δ ppm, $CDCl_3$): 7.68 (d, 1H, *J* = 16.20 Hz, C = CH), 7.45–7.59 (m, 5H, C = CH, Ar-H), 7.34–7.42 (m, 3H, Ar-H), 6.89 (d, 2H, *J* = 8.40 Hz, Ar-H), 6.67 (d, 1H, *J* = 16.20 Hz, CH = C), 6.43 (d, 1H, *J* = 15.60 Hz, CH = C), 5.42 (s, 1H, C_6-H), 4.71–4.79 (m, 1H, C_3α-H), 2.85 (m, 1H, C_{17}α-H), 1.04 (s, 3H, C_{10}-CH_3), 0.65 (s, 3H, C_{13}-CH_3). ^{13}C NMR (ppm, $CDCl_3$): 200.25, 166.41, 160.87, 144.47, 141.35, 139.72, 134.53, 130.18, 129.98(2C), 128.87(2C), 128.04(2C), 127.33, 124.63, 122.47, 118.68, 114.87(2C), 73.98, 63.64, 61.92, 57.15, 50.05, 44.93, 39.11, 38.21, 37.06, 36.68, 32.01, 31.89, 27.88, 24.71, 22.81, 21.10, 19.32, 14.73, 13.45. MS (ESI) (*m/z*): 553.2, 554.2 $[M + H]^+$. HRMS (EI): *m/z* $[M + Na]^+$ calcd for $C_{37}H_{41}FO_3$: 575.2937; found: 575.293141.

2.1.2.2.6. 3β-3-phenyl acrylates -pregn-5-en-17β-yl-3′-(p-tolyl)-phenylprop-2′-en-1′-one ***(11f)***. Yellow solid powder (Yield: 58.37%), M.p.: 188.2–189.7 °C. IR (KBr, cm^{-1}): 1708.30(C═O), 1679.80, 1644.25, 1604.25, 1585.0, 1487.06, 1450.53, 1174.51 (C—O), 1097.16 (C—O). ^1H NMR (600 MHz, δ ppm, $CDCl_3$): 7.68 (d, 1H, *J* = 16.20 Hz, C = CH), 7.49–7.56 (m, 3H, C = CH, Ar-H), 7.46 (d, 1H, *J* = 7.80 Hz, Ar-H), 7.33–7.41 (m, 3H, Ar-H),7.20 (d, 2H, *J* = 7.80 Hz, Ar-H), 6.75 (d, 1H, *J* = 16.20 Hz, CH = C), 6.43 (d, 1H, *J* = 16.20 Hz, CH = C), 5.42 (s, 1H, C_6-H), 4.71–4.79 (m, 1H, C_3α-H), 2.86 (m, 1H, C_{17}α-H), 2.38 (s, 3H, $C_{4''}$–CH_3), 1.04 (s, 3H, C_{10}-CH_3), 0.65 (s, 3H, C_{13}-CH_3).^{13}C NMR (ppm, $CDCl_3$): 200.38, 166.41, 144.48, 141.55, 139.72, 134.53, 132.09, 130.19, 129.66(2C), 128.87(2C), 128.30(2C), 128.04(2C), 127.12, 125.98, 122.46, 118.68, 73.98, 61.95, 57.15, 50.04, 44.96, 39.10, 38.21, 37.00, 36.64, 32.12, 31.95, 27.88, 24.70, 22.79, 21.49, 21.10, 19.35, 13.44. MS (ESI) (*m/z*): 549.3 $[M + H]^+$. HRMS (EI): *m/z* $[M + Na]^+$ calcd for $C_{38}H_{44}O_3$: 571.3188; found: 571.318145.

2.1.2.2.7. 3β-3-phenyl acrylates -pregn-5-en-17β-yl-3′-(m,p-dimethoxy)-phenylprop-2′-en-1′-one ***(11 g)***. Yellow solid powder (Yield: 75.23%), M.p.: 153.1–153.7 °C. IR (KBr, cm^{-1}): 1701.73(C═O), 1676.37, 1638.22, 1595.80, 1513.00, 1450.95, 1171.51 (C—O), 1098.15 (C—O). ^1H NMR (600 MHz, δ ppm, $CDCl_3$): 7.68 (d, 1H, *J* = 15.60 Hz, C = CH), 7.46–7.59 (m, 3H, C = CH, Ar-H), 7.34–7.43 (m, 3H, Ar-H), 7.16 (d, 1H, *J* = 6.0 Hz, Ar-H), 6.87 (d, 1H, *J* = 7.80 Hz, Ar-H), 6.66 (d, 1H, *J* = 16.20 Hz, CH = C), 6.43 (d, 1H, *J* = 16.20 Hz, CH = C), 5.42 (s, 1H, C_6-H), 4.72–4.78 (m, 1H, C_3α-H), 3.92 (s, 6H, $C_{3'',\ 4''}$–OCH_3), 2.88 (m, 1H, C_{17}α-H), 1.04 (s, 3H, C_{10}-CH_3), 0.66 (s, 3H, C_{13}-CH_3). ^{13}C NMR (ppm, $CDCl_3$): 200.24, 166.40, 151.22, 149.26, 144.48, 141.63, 139.71, 134.52, 130.19, 128.87(2C), 128.04(2C), 127.78, 125.11, 122.75, 122.45, 118.66, 111.16, 110.06, 73.96, 61.66, 57.17, 56.00 (2C), 50.06, 44.97, 39.08, 38.20, 37.07, 36.67, 32.01, 31.89, 27.88, 24.72, 22.91, 21.11, 19.35, 13.45. MS (ESI) (*m/z*):595.2 $[M + H]^+$. HRMS (EI): *m/z* $[M + Na]^+$ calcd for $C_{39}H_{46}O_5$: 617.3243; found: 617.323506.

2.1.2.2.8. 3β-3-phenyl acrylates -pregn-5-en-17β-yl-3′-(p-methylthio)-phenylprop-2′-en-1′-one ***(11 h)***. Light yellow solid powder (Yield: 72.44%), M.p.: 192.9–193.6 °C. IR (KBr, cm^{-1}): 1699.79(C═O), 1677.15, 1638.28, 1600.68, 1492.25, 1450.81, 1173.95 (C—O), 1089.88 (C—O). ^1H NMR (600 MHz, δ ppm, $CDCl_3$): 7.68 (d, 1H, *J* = 16.20 Hz, C = CH), 7.44–7.57 (m, 5H, C = CH, Ar-H), 7.35–7.43 (m, 3H, Ar-H),7.23 (d, 2H, *J* = 8.40 Hz, Ar-H), 6.73 (d, 1H, *J* = 16.20 Hz, CH = C), 6.43 (d, 1H, *J* = 16.20 Hz, CH = C), 5.42 (s, 1H, C_6-H), 4.73–4.78 (m, 1H, C_3α-H), 2.85 (m, 1H, C_{17}α-H), 2.51 (s, 3H, $C_{4''}$-SCH_3), 1.04 (s, 3H, C_{10}-CH_3), 0.65 (s, 3H, C_{13}-CH_3). ^{13}C NMR (ppm, $CDCl_3$):200.24, 166.41, 144.48, 141.95, 140.93, 139.72, 134.53, 131.36, 130.19, 128.87(2C), 128.64(2C), 128.04(2C), 126.07(2C), 125.90, 122.45, 118.67, 73.97, 62.04, 57.14, 50.03, 44.99, 39.11, 38.20, 37.06, 36.67, 32.01, 31.88, 27.88, 24.72, 22.80, 21.10, 19.35, 15.22, 13.44. MS (ESI) (*m/z*): 581.2 $[M + H]^+$. HRMS (EI): *m/z* $[M + Na]^+$ calcd for $C_{38}H_{44}O_3S$: 603.2909; found: 603.290271.

2.1.2.2.9. 3β-3-phenyl acrylates -pregn-5-en-17β-yl-3′-(o-fluoro)-phenylprop-2′-en-1′-one ***(11i)***. Yellow solid powder (Yield: 66.21%), M.p.: 174.5–177.5 °C. IR (KBr, cm^{-1}): 1703.24(C═O), 1683.15, 1642.85, 1612.38, 1577.17, 1482.15, 1455.34, 1173.27 (C—O), 1097.89 (C—O). ^1H NMR (600 MHz, δ ppm, $CDCl_3$):7.65–7.71 (m, 2H, C = CH), 7.57 (m, 1H, Ar-H), 7.48–7.53 (m, 2H, Ar-H), 7.34–7.41 (m, 4H, Ar-H), 7.17 (m, 1H, Ar-H), 7.10 (m, 1H, Ar-H), 6.88 (d, 1H, *J* = 15.60 Hz, CH = C), 6.43 (d, 1H, *J* = 15.60 Hz, CH = C), 5.42 (s, 1H, C_6-H), 4.71–4.79 (m, 1H, C_3α-H), 2.89 (m, 1H, C_{17}α-H), 1.04 (s, 3H, C_{10}-CH_3), 0.64 (s, 3H, C_{13}-CH_3). ^{13}C NMR (ppm, $CDCl_3$): 200.41, 166.39, 162.49, 160.81, 144.47, 139.72, 134.53, 134.11, 131.61, 130.19, 129.33, 128.87(2C), 128.04 (2C), 124.47, 122.95, 122.44, 118.68, 116.22, 73.97, 61.97, 57.12, 49.99, 44.98, 39.03, 38.21, 37.05, 36.67, 32.01, 31.87, 27.88, 24.69, 22.78, 21.10, 19.35, 13.48. MS (ESI) (*m/z*): 553.3, 554.3 $[M + H]^+$. HRMS (EI): *m/z* $[M + Na]^+$ calcd for $C_{37}H_{41}FO_3$: 575.2937; found:

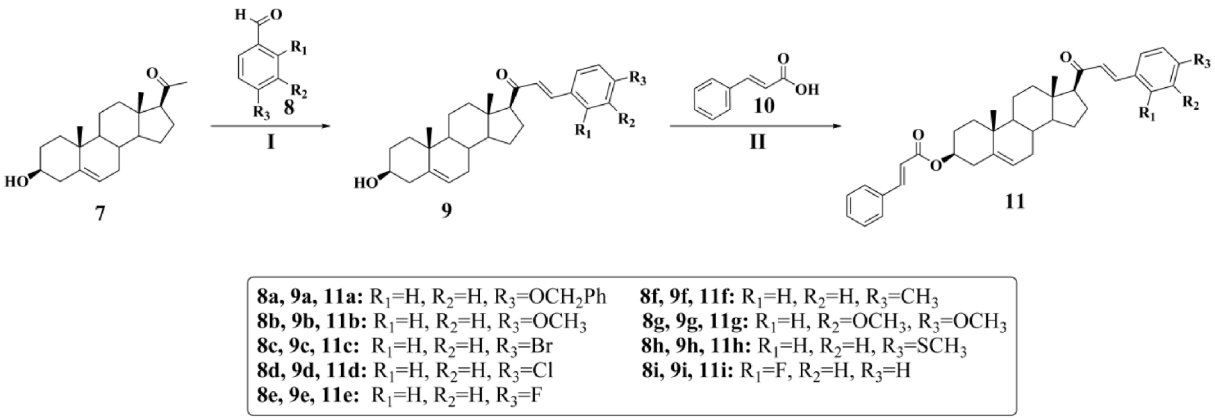

Scheme 1. General synthesis of compounds **11a–11i**.Reagents and conditions: (I) pregnenolone (0.01 mol), substituted benzaldehyde (0.012 mol), absolute ethanol, sodium hydroxide, room temperature 48 h, yield 75–86%; (II) dichloromethane, EDCI/DMAP, cinnamic acid, room temperature 48 h, yield 51–75%.

575.293075.

2.2. Biological methods

2.2.1. Cell culture and treatment

Primary cell culture was carried out as described previously [42]. RAW 264.7 cells (murine macrophage cell line) were purchased from Chinese Type Tissue Culture Collection (CTCC, Shanghai, China) and cultivated in H-DMEM (High Dulbecco modified Eagle medium, Sigma) containing 10% heat-inactivated 10% foetal bovine serum (FBS), 100 U/mL penicillin, and 100 μg/mL streptomycin at 37 °C in a humidified atmosphere of 95% air and 5% CO_2. Stock solutions of the compounds were prepared in dimethyl sulfoxide (DMSO) and then added to fresh culture medium to obtain the final concentrations. Unless stated otherwise, RAW 264.7 cells were plated at 1×10^4 cells per well in 96-well plates and incubated overnight to allow adherence to the plate prior to each of the experiments described below. For all experiments, LPS was used at a final concentration of 1 μg/mL. LPS (*Escherichia coli* 0111: B4) was purchased from Sigma (St. Louis, MO, USA).

2.2.2. Cell viability assay

Cell viability was determined using the 3 [4, 5-dimethylthiazol-2-yl]-2, 5-diphenyltetrazolium bromide (MTT) assay. The MTT assay was used to assess cell viability as described in our previous report [42]. Three micromolar concentrations of each compound were used to identify the more effective compounds for further study. Cell growth was arrested by incubation of the cells in 2% serum medium for 24 h before treatment. The indicated cells were then seeded in 96-well culture plates at a density of 5×10^3 cells/well and stimulated with different concentrations of compound **11e** (0, 0.1, 0.3, 1, 3, 10, or 30 μM/L) at 37 °C in 5% CO_2 saturated humidity conditions for 24 h. Finally, the optical density (OD) was measured at 570 nm with the aid of a FilterMax F3/F5 Microplate Reader (Molecular Devices, Sydney, Australia). The results are expressed as the ratio by normalizing the targeted OD level to that of the control OD.

2.2.3. Quantification of nitric oxide/nitrite

Nitrite that accumulated in the medium was measured as an indicator of NO production based on the Griess reaction. RAW 264.7 cells were seeded in 96-well plates at a density of 1×10^4 cells/well. The cells were pretreated with different concentrations of the test compounds **11a**, **11b**, **11c**, **11d**, and **11e** and **dexamethasone** dissolved in H-DMEM for 60 min before being stimulated with LPS (1 μg/mL) for 24 h. The cell culture medium was collected, and the concentration of nitrite was measured using the NO assay kit (Griess reagent) according to the manufacturer's instructions (Jiancheng Bioengineering Institute, Nanking, China). The absorbance at 540 nm was measured with a FilterMax F3/F5 Microplate Reader (Molecular Devices, Sydney, Australia).

2.2.4. Quantification of TNF-α, IL-6, and PGE-2

RAW 264.7 cells were treated with the indicated concentrations of compound **11e** dissolved in DMEM for 60 min, followed by incubation with 1 μg/mL LPS for 24 h. The cell culture medium was collected, and the levels of TNF-α, IL-6, and PGE-2 in the supernatants were determined by specific ELISA kits (Elabscience Biotechnology, Wuhan, China) according to the manufacturer's instructions. The cytokine concentration was measured by a FilterMax F3/F5 Microplate Reader (Molecular Devices, Sydney, Australia) at 450 nm and calculated from a standard curve prepared with the corresponding recombinant mouse cytokine.

2.2.5. Real-time quantitative PCR analysis

RAW 264.7 cells were seeded in 6-well plates at a density of 1×10^6 cells/well. The cells were preincubated with or without compound **11e** (1, 3, or 10 μM) for 60 min and then stimulated with LPS (1 μg/mL). After stimulation with LPS for 6 h, the cells were harvested, and total RNA was extracted using TRIzol reagent (Invitrogen, Shanghai, China). cDNA was prepared from total RNA (1 μg) using the High-capacity cDNA Reverse Transcription kit (Thermo Fisher Scientific, USA) according to the manufacturer's instructions. Real-time qRT-PCR was performed using the SYBR Green Supermix reagent (Thermo Fisher Scientific, USA) in a 7500 Real Time PCR system (Applied Biosystems, Foster City, CA, USA). The relative amount of gene expression was reported as a quantity relative to the control value by using the $2^{-\triangle\triangle Ct}$ method. The specific primer sets used have been previously reported [42].

2.2.6. Western blot analysis

RAW 264.7 cells were seeded in 6-well plates at a density of 1×10^6 cells/well. The cells were preincubated with or without compound **11e** (1, 3, or 10 μM) for 60 min and then stimulated with LPS (1 μg/mL). After stimulation with LPS for 24 h, whole cell protein (for COX-2, IL-1β, iNOS, and β-actin) and nuclear or cytoplasmic protein (for p65, IκBα, IKKβ, and β-actin) were extracted from the cells using Cell Lysis Reagent (Sigma) and ice cold lysis buffer (50 mM MHEPES, 400 mM KCl, 0.1 mM EDTA, 10% glycerol). The cell lysates (40 μg) were separated by SDS–PAGE, transferred to a nitrocellulose membrane and probed with anti-iNOS, COX-2 or IL-1β antibodies. β-actin was used as an internal control. The following primary and secondary antibodies were used for western blot analysis: primary antibodies against COX-2, IL-1β, iNOS, total and phospho-IκB, phospho-IKK, and β-actin and horseradish peroxidase-conjugated secondary antibodies. The antibodies were purchased from Abcam (Cambridge, MA).

Table 1
Inhibitory activity of compounds **11a** — **11i** (3 μM) on NO generation in LPS-induced RAW 264.7 cells [1].

Compounds	%Inhibition	%Cell viability	IC_{50}(μM)
11a	79.00 ± 1.34	89.94 ± 4.11	**1.54 ± 5.63**
11b	63.68 ± 4.17	98.59 ± 1.33	23.76 ± 4.37
11c	74.53 ± 6.81	67.96 ± 1.64	13.75 ± 6.21
11d	79.06 ± 0.75	88.57 ± 3.26	25.30 ± 8.25
11e	90.93 ± 0.85	101.15 ± 2.93	**1.46 ± 3.66**
11f	44.94 ± 9.31	88.00 ± 5.05	–
11 g	13.17 ± 3.80	84.85 ± 2.94	–
11 h	6.84 ± 8.31	88.07 ± 4.71	–
11i	58.08 ± 2.61	68.97 ± 1.00	**6.84 ± 5.17**
dexamethasone	92.34 ± 2.06	95.09 ± 1.78	0.62 ± 4.17

note: [1]Each experiment was independently performed three times.
note: "—": Not determined.

2.2.7. Molecular docking

Compound **11e** was docked with the target proteins (iNOS, COX-2, TNF-α, IL-1β, and IL-6) to confirm its anti-inflammatory potential. AutoDock 4.2.6 and AutoDock Vina 1.1.2 were used for molecular docking based on Lamarkian Genetic Algorithm [43]. Three-dimensional structure for compound **11e** was generated using Chem-draw 3D. Three-dimensional structures of the target proteins, iNOS (PDB ID: 4CX7), COX-2 (PDB ID: 5IKQ), TNF-α (PDB ID: 3ALQ), IL-1β (PDB ID: 1ITB), IL-6 (PDB ID: 1ALU), were retrieved from the Protein Data Bank (PDB) (http://www.pdb.org). Compound **11e** was docked to target protein complexes with the molecule considered as a rigid body and the ligands being flexible. The search was extended over the whole receptor protein used as blind docking. PyMOL molecular graphics system was applied to visualize the interactions between ligands and receptors.

2.2.8. Statistical analysis

The experimental values are presented as Mean ± SD, and statistical analysis were conducted by Statistical Product and Service Solutions (SPSS) 17.0 (SPSS Inc., Chicago, IL, USA) through one-way ANOVA detected by SNK-LSD test as the post-hoc test. $P < 0.05$ was considered statistically significant.

3. Results and discussion

3.1. Chemistry

The synthesis of highly functional molecules from simple building blocks has always attracted the attention of synthetic chemists. Here, we report the convenient and efficient synthesis of novel steroidal chalcones with 3β-pregnenolone esters of cinnamic acid derivatives involving aldol condensation as the first step followed by Steglich esterification as a later step. The synthesis of compounds **9a–9i** and **11a–11i** is presented in Scheme 1. First, chalcone derivatives **9** were prepared via a Claisen-Schmidt condensation reaction with the corresponding pregnenolone **7** and aromatic aldehyde **8**. NaOH was used as a catalyst in the reaction to obtain **9** (**9a-9i**). The further esterification of these molecules with cinnamic acid **10** in dry dichloromethane in the presence of EDCI and DMAP at room temperature (48 h) afforded moderate yields of the corresponding esters **11** (**11a–11i**). The structures of compounds **11a–11i** were determined by ^{1}H NMR, ^{13}C NMR, HRMS and IR analyses.

3.2. Evaluation of the effects of compounds *11a-11i* on NO generation in LPS-induced RAW264.7 cells and cell viability in vitro

NO has been identified as a pro-inflammatory molecule in the development of various inflammatory diseases. The production of NO is widely considered a hallmark of macrophage activation, which is indispensable for the pathogenesis of inflammatory diseases [44]. Activated macrophages can stimulate iNOS expression to generate NO in culture medium. To identify the most promising anti-inflammatory agent among the synthesized derivatives (**11a–11i**), the inhibitory effects of these derivatives on NO generation were tested in LPS-induced RAW 264.7 cells; **dexamethasone** was used as a positive control. The results showed that most of the novel synthetic compounds exhibited modest to strong inhibitory effects on NO generation at 3.0 μM (Table 1). Moreover, the cytotoxicity of the compounds was determined by MTT assay to exclude the possibility that the reduced release of NO was caused by the cytotoxic effects of the compounds (Table 1 and Fig. 2).

Compounds **11a** and **11e** exhibited IC_{50} values lower than 2.0 μM against LPS-induced RAW 264.7 cells at 24 h. The most effective agent was compound **11e**, with an IC_{50} value of 1.46 μM at 24 h. The test compounds also displayed dose-dependent trends. The results showed that compounds with an aromatic ring bond with electron-withdrawing groups exhibited moderate to strong inhibitory activity (**11d < 11c < 11i < 11e**). The introduction of an F, Cl group at the R_3 position resulted in increased inhibitory potency. With the introduction of an F group at the R_1 position, the inhibitory potency decreased significantly (**11i**) when compared to **11e**. However, compounds with an aromatic ring bond with electron-donating groups showed inferior inhibitory activity (**11b, 11f, 11 g,** and **11 h**).

No obvious toxicity was observed for compounds **11d** and **11e** (Fig. 2), in which R_3 was a Cl or F group. The R_3 position with a benzyloxy group brings obvious toxicity (**11a**). In the case in which the F substituent was changed from the R_3 position to the R_1 position, cytotoxicity was also increased (**11i**). A halogen substituent group for R_3 was effective, as compounds **11c, 11e,** and **11i** all showed good inhibitory activity. We also found that most of these 3β-pregnenolone esters of cinnamic acid derivatives showed lower toxicity than the D-ring heterocycle derivatives that we previously reported [42], and this lower toxicity may be related to the C-3 position (–OH) substituent.

Compounds **11a, 11b, 11c, 11d, 11e** and **11i,** which strongly suppressed LPS-induced NO generation and had low cytotoxicity in RAW 264.7 cells, were chosen for a concentration-dependent experiment in LPS-induced RAW 264.7 cells (Fig. 2). Compounds **11a** and **11e** were found to be the most potent, with an IC_{50} value of 1.54 and 1.46 μM, respectively, but lower than **dexamethasone**, with IC_{50} values of 0.62 μM (Table 1 and Fig. 2). Due to its strong inhibitory activity on NO generation and minimal cytotoxicity to RAW 264.7 cells, compound **11e** was selected for further evaluation.

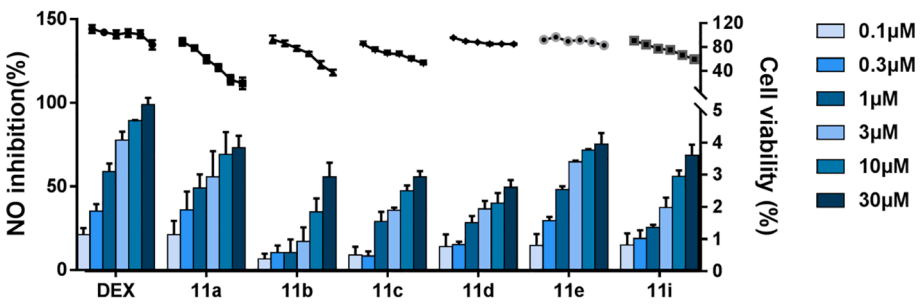

Fig.2. The effects of compound **11a, 11b, 11c, 11d, 11e, 11i** and **dexamethasone** on NO production and cell viability in LPS-induced RAW 264.7 cells. RAW 264.7 cells were pretreated with various concentrations (0.1, 0.3, 1, 3, 10 and 30 μM/L) of compound **11a, 11b, 11c, 11d, 11e, 11i** and **dexamethasone** for 60 min and then stimulated with LPS (1 μg/mL) for 24 h. The MTT assays results are expressed as a percentage of the respective control. Data shown are the mean ± SD for each group (n = 3) and are representative of three independent experiments.

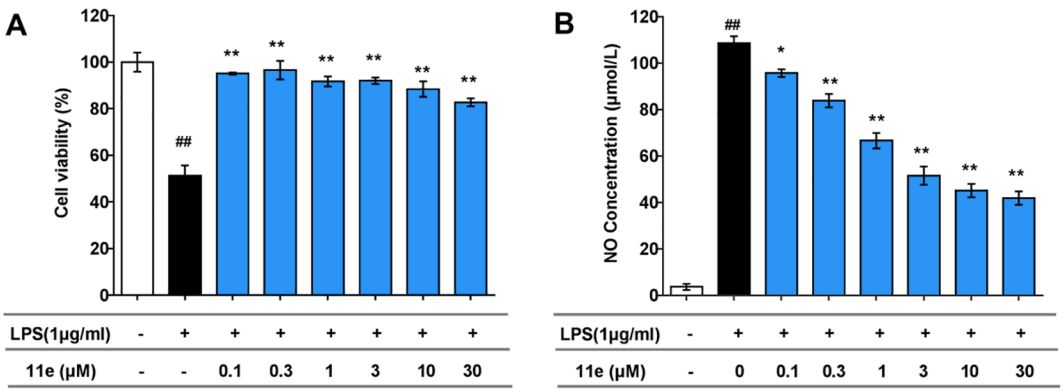

Fig.3. Cell viability of compound **11e** in RAW 264.7 cells. Cells were incubated with the indicated concentrations of compound **11e** (0, 0.1, 0.3, 1, 3, 10 and 30 μM/L) for 60 min and then stimulated with LPS (1 μg/mL) for 24 h. The results are expressed as a percentage of the respective control (A). The effect of compound **11e** on NO production in LPS-induced RAW 264.7 cells. RAW 264.7 cells were pretreated with various concentrations of compound **11e** for 60 min and then stimulated with LPS (1 μg/mL) for 24 h (B). Data shown are the mean ± SD for each group (n = 3) and are representative of three independent experiments ($^{*}P < 0.05$ and $^{**}P < 0.01$ vs. the LPS group; $^{\#\#}P < 0.01$ vs. the control group). Data were analysed by ANOVA and Duncan's multiple range tests.

3.3. Cytotoxic effects of compound *11e* on cell viability

Inflammation can be defined as the orchestrated response of inflammatory mediators, such as pro-inflammatory cytokines (TNF-α, IL-6, and IL-1), prostaglandin, and the free radical NO, against tissue injury or infection. Prior to the determination of the potential anti-inflammatory activity of compound **11e**, the cytotoxic effect of compound **11e** on LPS-induced inflammation was assessed in RAW 264.7 cells. As shown in Fig. 3A, the determination of optical density by MTT assay showed that 24 h LPS treatment significantly decreased the proliferation of RAW 264.7 cells compared to that of control cells, and the application of LPS with compound **11e** had no obvious effect on the proliferation of RAW 264.7 cells. However, 0.1–30 μM/L compound **11e** increased the cell viability of LPS-stimulated RAW 264.7 cells compared to the group receiving LPS treatment alone. As a result, compound **11e** did not show any cytotoxicity at concentrations up to 30 μM, whereas 10 μM and 30 μM compound **11e** slightly reduced cell viability in the presence of 1 μg/mL LPS (Fig. 3A).

3.4. Effects of compound *11e* on the production of NO

Although NO is responsible for host defence mechanisms, a high concentration of NO can cause toxicity and damage host cells. Excessive NO production is associated with the pathogenesis of inflammatory diseases, including atherosclerosis, vascular disease and septic shock [44]. Nitric oxide is synthesized by iNOS and COX-2. Overexpression of both iNOS and COX-2 is commonly associated with inflammation. Therefore, the production of NO and the expression of iNOS and COX-2 can be important targets in the treatment or control of inflammation. To investigate the anti-inflammatory effects of compound **11e** in LPS-induced RAW 264.7 cells, the NO levels were determined (Fig. 3B). NO production was almost undetectable in cells without LPS stimulation (Fig. 3B). Exposure to 1 μg/mL LPS significantly increased NO production in RAW 264.7 cells compared to the control group, and compound **11e** significantly reduced the LPS-induced level of NO production in the cells. Treatment with 0.3–30 μM compound **11e** markedly reduced the LPS-mediated NO production by 29.43 ± 2.14%, 48.23 ± 1.60%, 64.70 ± 2.64%, 71.76 ± 4.51%, and 75.37 ± 5.90%. This result indicates that compound **11e** maximally inhibits NO generation by activated RAW 264.7 cells.

3.5. Effects of compound *11e* on the production of IL-6, PGE-2, and TNF-α

The *in vitro* anti-inflammatory effect of compound **11e** was evaluated by determining the decrease in IL-6, PGE-2 and TNF-α in activated RAW 264.7 cells. The levels of these inflammatory cytokines were analysed using ELISA kits. LPS treatment alone resulted in a significant increase ($P < 0.01$) in cytokine production by RAW 264.7 cells compared with the control group (Fig. 4). Furthermore, pretreatment with higher concentrations of compound **11e** (3 and 10 μM) reduced the levels of IL-6 and PGE-2. As shown in Fig. 4, treatment with compound **11e** led to a decrease in PGE-2 from 451.86 ± 21.17 to 262.82 ± 22.04 pg/mL ($P < 0.01$) and 451.86 ± 21.17 to 254.20 ± 8.16 pg/mL ($P < 0.01$) , corresponding to a decrease in IL-6 from 224.94 ± 6.03 to 180.76 ± 1.48 pg/mL ($P < 0.01$) and 224.94 ± 6.03 to 167.78 ± 1.46 pg/mL ($P < 0.01$).

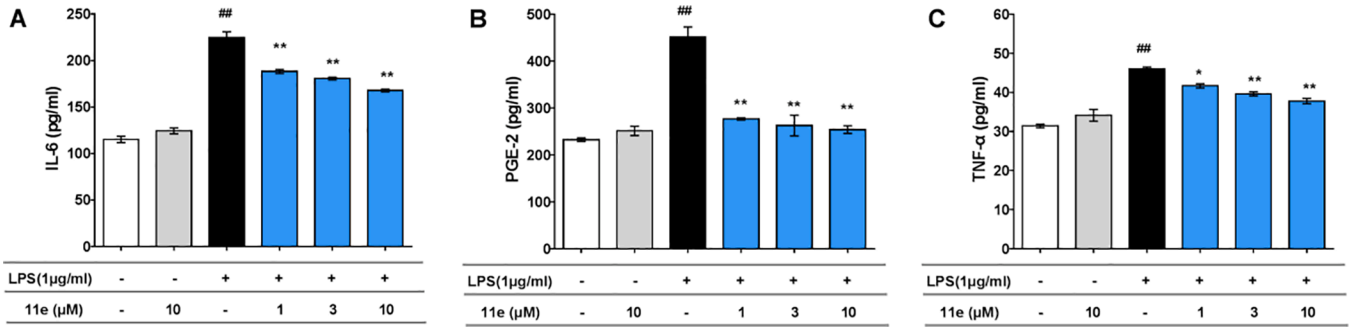

Fig.4. Effect of compound **11e** on IL-6 (A), PGE-2 (B) and TNF-α (C) release in LPS-induced RAW 264.7 cells. RAW 264.7 cells were preincubated with different concentrations of compound **11e** (0, 1, 3, or 10 μM/L) for 60 min prior to LPS stimulation. After treatment with LPS for 24 h, cell culture medium was collected, and ELISA was performed to assess the levels of inflammatory cytokines. The values are presented as the mean ± S.D. (n = 3) of three independent experiments. ($^{*}P < 0.05$ and $^{**}P < 0.01$ vs. the LPS group; $^{\#\#}P < 0.01$ vs. the control group).

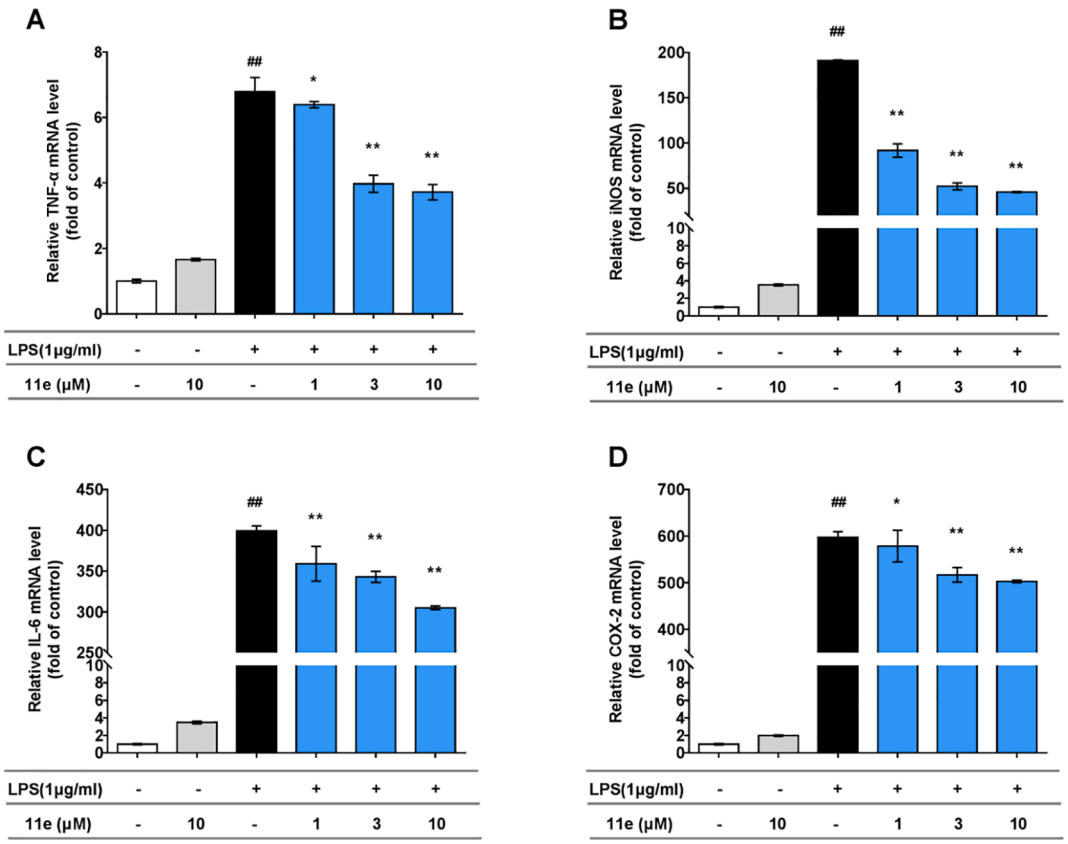

Fig.5. Effects of compound **11e** on the mRNA levels of TNF-α, iNOS, IL-6 and COX-2 in LPS-induced RAW 264.7 cells. RAW 264.7 cells were preincubated with different concentrations of compound **11e** (0, 1, 3, or 10 μM/L) for 60 min prior to LPS stimulation. After treatment with LPS (1 μg/mL) for 6 h, total RNA was isolated, and iNOS (B) and mRNA levels of TNF-α (A), IL-6 (C) and COX-2 (D) were determined by quantitative RT-PCR. The data are representative of three independent experiments. ($^{*}P < 0.05$ and $^{**}P < 0.01$ vs. the LPS group; $^{\#\#}P < 0.01$ vs. the control group).

Incubation with high doses of compound **11e** effectively downregulated the production of IL-6 and PGE-2 in a dose-dependent manner. However, compound **11e** produced a much weaker inhibitory effect on TNF-α production. Briefly, compound **11e** treatment exerted an inhibitory effect on the IL-6, PGE-2, and TNF-α expression levels in activated RAW 264.7 cells.

3.6. *Effects of compound **11e** on the expression of genes encoding pro-inflammatory proteins*

Inflammatory cytokines, including TNF-α, iNOS, IL-6 and COX-2, are also associated with inflammatory disorders. Therefore, we tested whether compound **11e** inhibited the transcriptional expression of these cytokines and inflammatory enzymes using quantitative real-time (RT)-PCR analysis. The stimulation of RAW 264.7 macrophages with LPS remarkably increased the mRNA levels of TNF-α (Fig. 5A), iNOS (Fig. 5B), IL-6 (Fig. 5C) and COX-2 (Fig. 5D). Similar to the ELISA

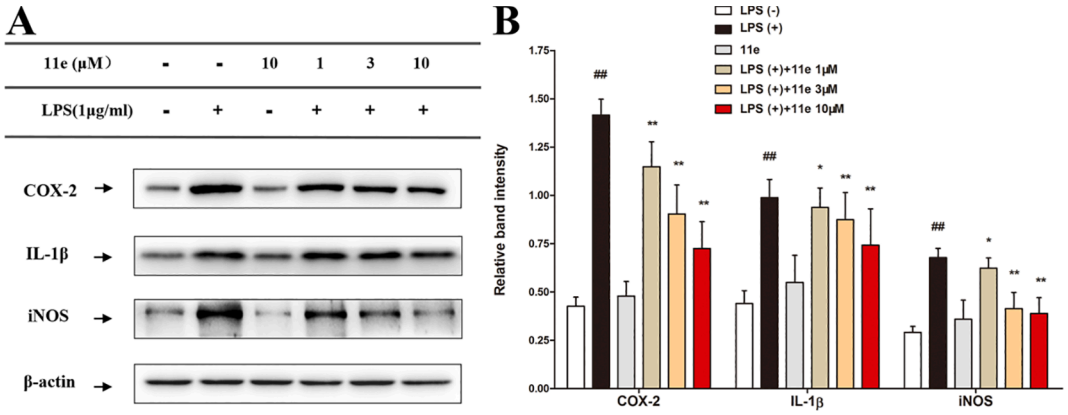

Fig.6. Effects of compound **11e** on LPS-induced expression of COX-2, IL-1β and iNOS proteins. (A, B) Compound **11e** reduced the protein expression of COX-2, IL-1β and iNOS in LPS-induced RAW 264.7 cells. RAW 264.7 cells were preincubated with the indicated concentrations of compound **11e** (0, 1, 3, or 10 μM/L) for 60 min and then stimulated with LPS for 24 h. Total protein was extracted and subjected to western blot analysis to detect the COX-2, IL-1β and iNOS proteins. The data are representative of three independent experiments. ($^{*}P < 0.05$ and $^{**}P < 0.01$ vs. the LPS group; $^{\#}P < 0.05$ and $^{\#\#}P < 0.01$ vs. the control group).

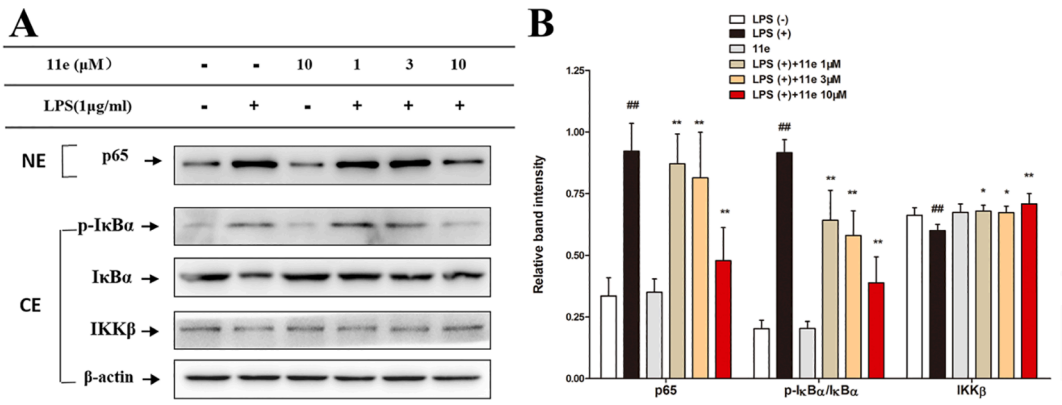

Fig.7. Compound **11e** suppressed the expression of inflammatory mediators by inhibiting NF-κB signalling in RAW 264.7 cells. (A, B) Compound **11e** reduced LPS-induced NF-κB signalling in RAW 264.7 cells. RAW 264.7 cells were preincubated with the indicated concentrations of compound **11e** (0, 1, 3, or 10 μM/L) for 60 min and then stimulated with LPS for 24 h. Nuclear extracts (NE) and cytosolic extracts (CE) were used for western blot analyses. The data are representative of three independent experiments. ($^{*}P < 0.05$ and $^{**}P < 0.01$ vs. the LPS group; $^{\#\#}P < 0.01$ vs. the control group).

results, compound **11e** markedly prevented the LPS-induced production of TNF-α, iNOS, IL-6 and COX-2 protein in a dose-dependent manner. These findings indicated that compound **11e** exerted significant anti-inflammatory effects in LPS-induced RAW 264.7 cells by suppressing the mRNA and protein expression of TNF-α, iNOS, IL-6 and COX-2.

*3.7. Effects of compound **11e** on COX-2, IL-1β and iNOS protein expression*

iNOS in macrophages may produce excessive NO to exert toxic effects on cells in response to inflammatory stimuli, such as LPS and cytokines. It is accepted that macrophages may induce the expression of inflammatory enzymes, such as iNOS and COX-2, during inflammatory responses [44]. Compound **11e** significantly reduced the expression of COX-2, IL-1β and iNOS mRNAs, and we therefore determined their protein levels to further investigate this anti-inflammatory effect. As revealed in Fig. 6, in response to LPS, the levels of these proteins were upregulated. In contrast, pretreatment with compound **11e** obviously inhibited the upregulation in COX-2, IL-1β and iNOS protein expression. The significant increases in COX-2, IL-1β and iNOS protein levels observed in LPS-induced RAW 264.7 cells were markedly reduced by treatment with 3 or 10 μM compound **11e** (Fig. 6A-6B). These findings indicated that compound **11e** exerted significant anti-inflammatory effects in LPS-induced RAW 264.7 cells by suppressing the mRNA and protein expression of COX-2, IL-1β and iNOS.

*3.8. Effects of compound **11e** on NF-κB signalling*

NF-κB is an important transcription factor that regulates the expression of inflammatory mediators. Nucleus translocation of p65-NF-κB is considered a prerequisite for transcription [45]. The phosphorylation of IκBα is upstream of p65-NFκB translocation. The activation of IKKβ is crucial for the phosphorylation of IκBα and the translocation of NFκB in a canonical pathway. To assess whether the inhibitory effects of compound **11e** on COX-2, IL-1β and iNOS expression were mediated by NF-κB, we examined the effects of compound **11e** on the LPS-induced expression of NF-κB p65 and on the degradation of the upstream proteins IκBα and IKKβ. The expression levels of NF-κB p65 were determined by western blot using the nuclear and cytosolic extracts of RAW 264.7 cells. The NF-κB p65 protein was markedly increased after exposure to LPS. However, this increase was alleviated in the cells treated with 3 or 10 μM compound **11e** (Fig. 7A-7B). Exposure of RAW 264.7 cells to LPS significantly increased the phosphorylation of IκBα in RAW 264.7 cells, whereas compound **11e** markedly inhibited the LPS-induced phosphorylation of IκBα. Moreover, compound **11e** attenuated the LPS-induced degradation of IκBα and IKKβ (Fig. 7A-7B). These results suggest that the LPS-stimulated activation of NF-κB might be blocked by compound **11e**.

Table 2
Docking score (kcal/mol) of potential active compounds **11a-11i** and standard drug **dexamethasone** to five target proteins.

Compounds	Target proteins				
	iNOS	COX-2	TNF-α	IL-1β	IL-6
11a	−13.2	−10.4	−8.1	−9.2	−9.1
11b	12.7	−10.1	−7.6	−8.9	−8.2
11c	−12.0	−10.3	−8.2	−8.9	−8.2
11d	−12.4	−10.4	−8.0	−9.3	−8.5
11e	−13.9	−11.1	−8.6	−9.3	−8.1
11f	−13.8	−10.9	−8.1	−9.2	−8.4
11 g	−12.3	−9.7	−7.7	−8.9	−8.3
11 h	−12.3	−10.0	−7.9	−8.6	−8.4
11i	−13.9	−11.5	−7.8	−9.0	−8.7
dexamethasone	−8.7	−8.2	−6.7	−6.5	−6.6

3.9. Molecular docking analysis

The binding affinity of a ligand to a target is indispensable for tight association, to attenuate the drug concentration and to lower the risk of side effects engendered by nonspecific or nontarget binding during treatment [46,47]. *In vitro* anti-inflammatory profiles of steroidal chalcones with 3β-pregnenolone esters were further confirmed by molecular docking experiments. This molecular docking study aimed to rationalize and verify the obtained biological data and to explain the possible interactions of the derivatives with the crystal structures of the iNOS (4CX7), COX-2 (5IKQ), TNF-α (3ALQ), IL-1β (1ITB), and IL-6 (1ALU) enzymes. The interaction study was compared with **dexamethasone**, a standard steroidal anti- inflammatory drug.

The docking scores (kcal/mol) of potential active compounds **11a-11i** and the standard drug **dexamethasone** to five target proteins are shown in Table 2. The autodock results of the synthesized compounds into the binding site of iNOS revealed that compounds **11a**, **11e**, **11f** and **11i** exhibited the highest binding affinities through their lowest binding free energies of −13.2, −13.9, −13.8 and −13.9 kcal/mol, respectively. These derivatives also displayed at least fourteen hydrophobic bonds with the key amino acids of iNOS. On the other hand, the autodock results of the synthesized compounds into the binding site of COX-2 revealed that compounds **11e**, **11f** and **11i** exhibited very high binding affinities through their very low binding free energies of −11.1, −10.9 and −11.5 kcal/mol, respectively. These compounds also displayed at least fifteen hydrophobic bonds with the key amino acids of COX-2. Compounds **11e** and **11i** displayed one hydrogen bond with the

Table 3
Structure-activity relationship of potent compounds (**11a, 11e, 11i**) with inflammatory biomarkers iNOS, COX-2, TNF-α, IL-1β and IL-6 and standard drug **dexamethasone**, respectively.

Target protein and (PDB ID)	Ligand molecule	Amino acid residues on docked domains
iNOS (4CX7)	**11a**	Ile462, Gln263, Glu377, Val352, Trp194, Asn370, Leu209, Tyr489, Phe369, Gly371, Pro350, Arg381, Pro467, Val465
	11e	Tyr489, Arg381, Glu377, Met374, Gly371, Asn370, Val352, Phe369, Leu209, Trp194, Arg199, Met120, Ile462, Trp463, Ile201, Pro466, Pro467
	11i	Leu209, Trp194, Gly371, Pro350, Glu377, Ile201, Met374, Pro467, Pro466, Trp463, Ile462, Arg381, Met120, Arg199, Cys200, Tyr489, Asn370, Phe369, Val352
	Dexamethasone	Glu377, Trp372, Ile201, Trp463, Met120, Arg381, Pro467, Cys200, Met374, Arg199
COX-2 (5IKQ)	**11a**	Leu294, His214, His207, Val295, His386, Tyr385, Gln203, Ala199, Phe200, Leu391, Tyr404, Phe395, Val444, Ile408
	11e	Gln289, Glu290, Lys211, Thr212, His214, Phe210, Tyr385, Val447, His388, Trp387, Ala202, Thr206, His207, Gln203, Val291, Ile274
	11i	Gln289, Ile274, Glu290, Val291, Thr212, His388, His207, Val447, Gln203, Leu390, Ala202, Trp387, Tyr385, Thr206, Phe210, Lys211
	Dexamethasone	Arg376, Val538, Gly536, Asn375, Gly225, Val228, Gly227, Asn537, Tyr373, Gln374, Phe142
TNF-α (3ALQ)	**11a**	Ile136, Gln27, Asp45, Leu43, Arg31, Leu37, Glu135, Glu42, Asn30, Trp28, Asn46, Pro139, Leu26
	11e	Phe144, Ala145, Glu146, Ser147, Val150, Gly148, Val17, Arg32, Ala18, Pro20
	11i	Phe144, Ala145, Gln67, Leu142, Arg138, Tyr141, Asp140, Gly66, Ser65, Asp143, Glu23, Gln21, Pro20
	Dexamethasone	Gly24, Asp143, Ser65, Tyr115, Phe144, Leu142, Gln67, Gly66, Asp140, Glu23
IL-1β (1ITB)	**11a**	Asp142, Phe133, Pro131, Gln81, Val132, Leu82, Ser84, Glu83, Tyr24, Leu80, Glu25, Ser125, Ala127
	11e	Pro131, Glu25, Tyr24, Ser84, Glu83, Leu82, Gln81, Leu80, Phe133, Val132
	11i	Pro131, Leu80, Gln81, Glu83, Ser84, Tyr24, Leu82, Glu25, Phe133, Val132
	Dexamethasone	Leu80, Tyr24, Pro131, Gln81, Val132, Leu82, Glu25, Thr79, Phe133
IL-6 (1ALU)	**11a**	Arg30, Tyr31, Val115, Ala114, Gln111, Gly35, Asp34, Ser37, Lys171, Leu33
	11e	Lys27, Tyr31, Gln111, Gly35, Glu110, Ala114, Ser118, Val121, Gln28
	11i	Lys120, Ala114, Val115, Ile32, Tyr31, Gly35, Glu110, Met117, Gln111, Arg113, Ser118, Val121
	Dexamethasone	Arg179, Arg182, Leu33, Leu178, Gln175, Arg30

key amino acids of COX-2, Gln289 (Table 3).

The anti-inflammatory potential of compound **11e** was confirmed by its binding potency to pro-inflammatory cytokines. The docked poses of compound **11e** with target proteins (iNOS, COX-2, TNF-α, IL-1β, and IL-

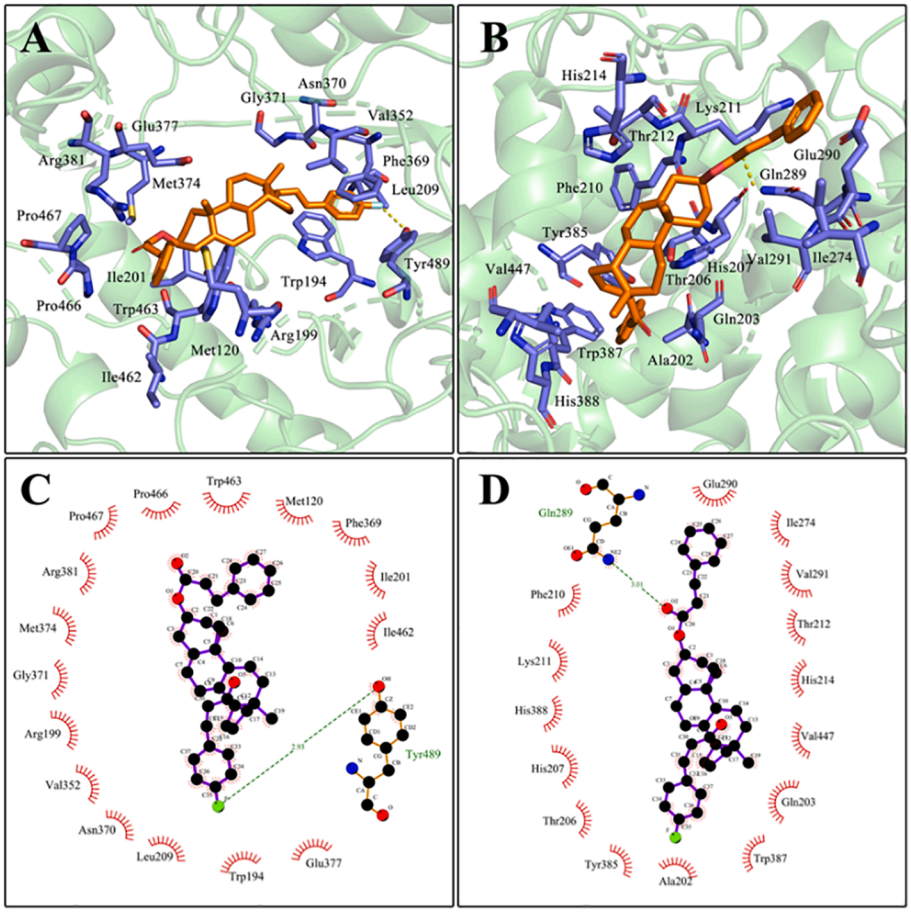

Fig.8. The docked poses of compound **11e** (colored orange) on iNOS (PDB ID: 4CX7) and COX-2 (PDB ID: 5IKQ) proteins' binding site. Targeted proteins are shown in cartoon forms and portrayed in green. Amino acid residues near this site are shown as sticks and carbons are portrayed in blue. Fluorine is displayed in light blue. The yellow dashed lines represent hydrogen bonds. Besides it, the 2D representations of each docked pose and their interactions are shown. (A) 3D docking diagram of compound **11e** and iNOS. (B) 3D docking diagram of compound **11e** and COX-2. (C) 2D docking diagram of compound **11e** and iNOS. (D) 2D docking diagram of compound **11e** and COX-2.

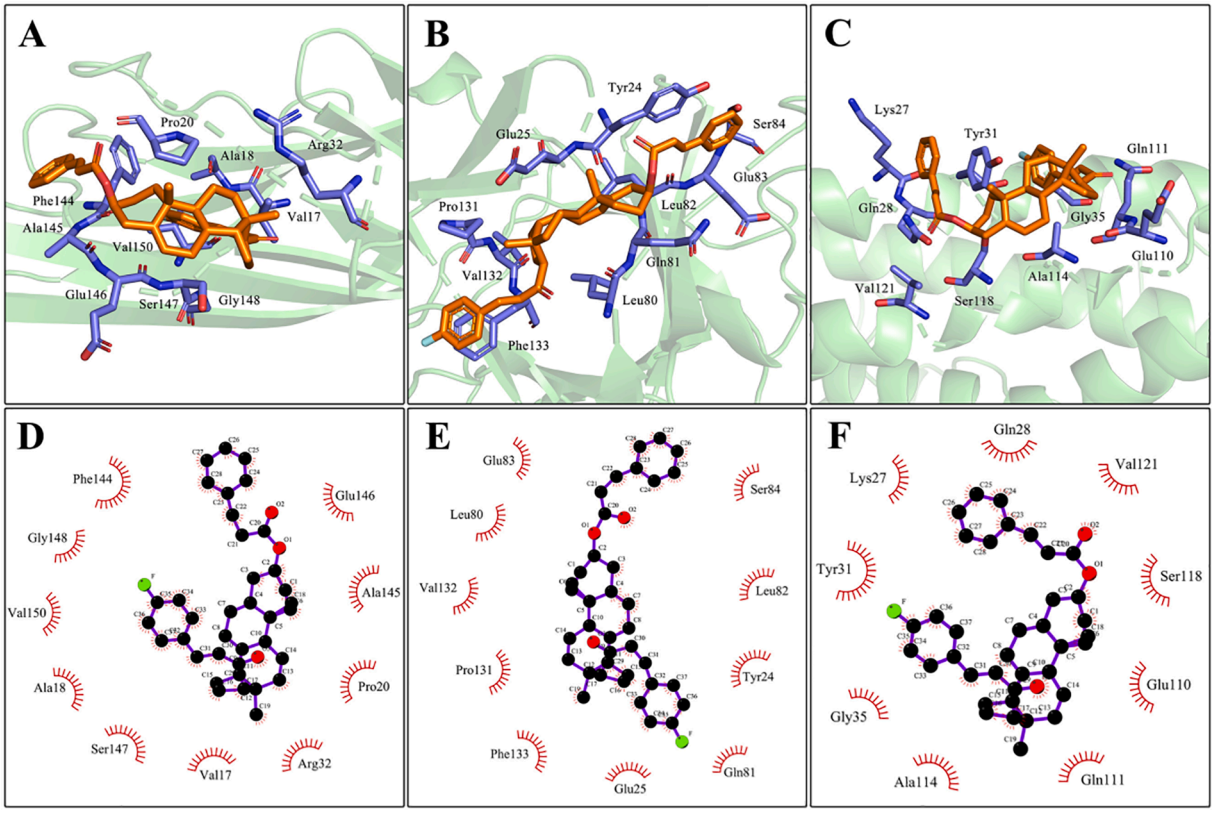

Fig.9. The docked poses of compound **11e** on TNF-α (PDB ID: 3ALQ), IL-1β (PDB ID: 1ITB) and IL-6 (PDB ID: 1ALU) proteins' binding site. (A) 3D docking diagram of compound **11e** and TNF-α. (B) 3D docking diagram of compound **11e** and IL-1β. (C) 3D docking diagram of compound **11e** and IL-6. (D) 2D docking diagram of compound **11e** and TNF-α. (E) 2D docking diagram of compound **11e** and IL-1β. (F) 2D docking diagram of compound **11e** and IL-6.

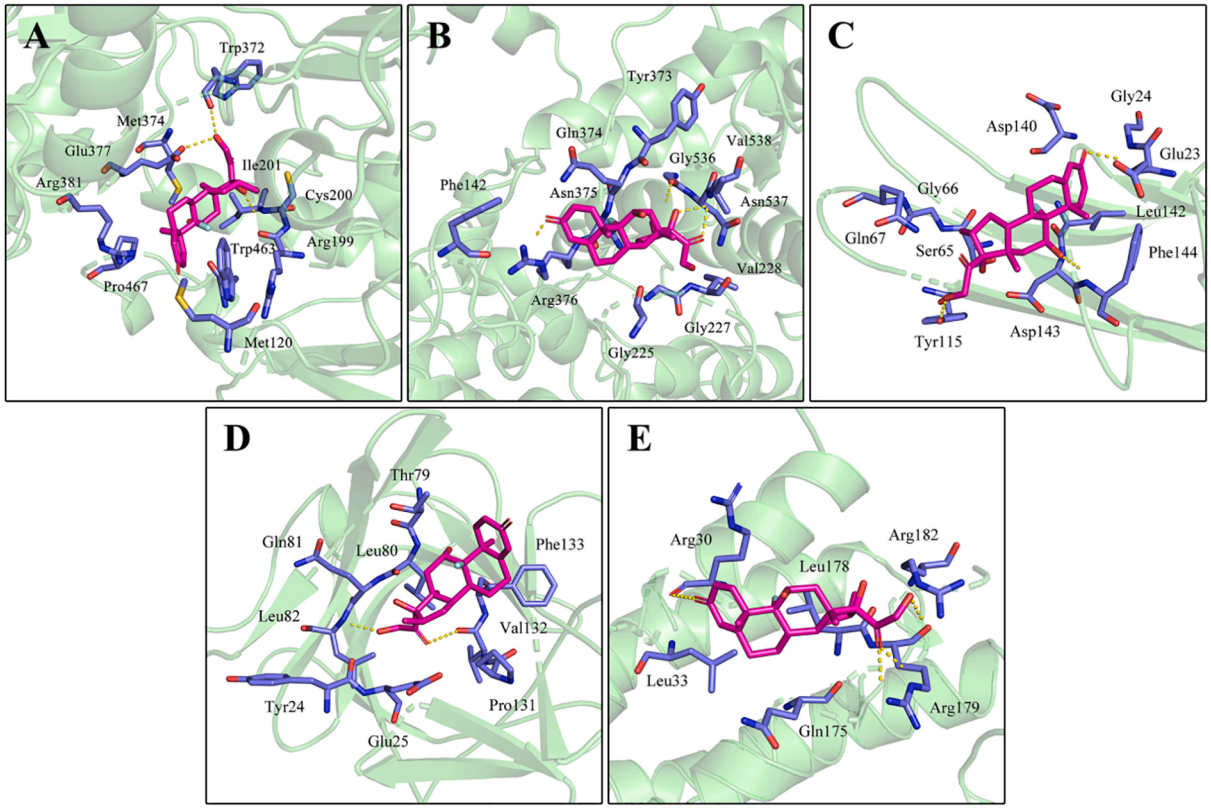

Fig.10. The docked poses of **dexamethaone** (colored rose red) on iNOS (PDB ID: 4CX7), COX-2 (PDB ID: 5IKQ), TNF-α (PDB ID: 3ALQ), IL-1β (PDB ID: 1ITB) and IL-6 (PDB ID: 1ALU) proteins' binding site. (A) 3D docking diagram of **dexamethaone** and iNOS. (B) 3D docking diagram of **dexamethaone** and COX-2. (C) 3D docking diagram of **dexamethaone** and TNF-α. (D) 3D docking diagram of **dexamethaone** and IL-1β. (E) 3D docking diagram of **dexamethaone** and IL-6.

6) are shown in Fig. 8 and Fig. 9. The binding profile of compound **11e** docked with iNOS and COX-2 showed binding energies of −13.9 and −11.1 kcal/mol, respectively. Ligand **11e** docks into the active sites of iNOS successfully, produces deep movement into the hydrophilic (Tyr489) pockets of the receptor and binds to hydrophobic amino acids (Arg381, Glu377, Met374, Gly371, Asn370, Val352, Phe369, Leu209, Trp194, Arg199, Met120, Ile462, Trp463, Ile201, Pro466 and Pro467), indicating that such interactions are almost essential for iNOS inhibitory activity (Fig. 8A, 8C). Compound **11e** also forms one hydrogen bond with Gln289 of COX-2, and 15 binds to hydrophobic amino acids (with residues Glu290, Lys211, Thr212, His214, Phe210, Tyr385, Val447, His388, Trp387, Ala202, Thr206, His207, Gln203, Val291 and Ile274) (Fig. 8B, 8D). The docking and binding affinity of compound **11e** into the iNOS active site are shown in Fig. 8, where **11e** exhibited one hydrogen bond between its F group and the OH of Tyr489.Additionally, the docking and binding affinity of compound **11e** into the COX-2 active site exhibited one hydrogen bond between its C═O group and the NH_2 of Gln289. Compound **11e** showed better anti-inflammatory activities than the other synthesized compounds as they exhibited lower binding free energies. The main interactions of compound **11e** with the TNF-α, IL-1β, and IL-6 enzymes were hydrophobic effects (Fig. 9). However, compound **11e** is highly actively docked with iNOS and COX-2, and this high binding affinity may be due to the -F and -COOR chains. Previous literatures have been reported that the introduction of fluorine atoms may affect the binding strength of molecular ligands and substrate proteins. Fluorine atoms can increase the lipophilicity of molecules, which make it easier to pass through the lipid cell membrane, and then improve the cell activity [48,49].

The main interactions of the standard drug **dexamethasone** with the five enzymes were investigated. The hydroxy group of **dexamethasone** exhibited three hydrogen bonds with the key amino acids of iNOS: Glu377, Trp372 and Ile201. Additionally, other residues in the binding pocket may be involved in such interactions, including Trp463, Met120, Arg381, Pro467, Cys200, Met374 and Arg199 as shown in Fig. 10, whereas, the main amino acids involved in COX-2 interaction with the ligand **dexamethasone** are Asn375, Gly225, Val228, Gly227, Asn537, Tyr373, Gln374 and Phe142. Arg376, Val538 and Gly536 form three hydrogen bonds with the ligand **dexamethasone**. The main amino acids involved in TNF-α, IL-1β, and IL-6 interactions with the ligand **dexamethasone** are shown in Fig. 10.

Table 3 depicts the structure–activity relationship of potent compounds (**11a, 11e, 11i**) and the standard drug **dexamethasone** with the inflammatory biomarkers iNOS, COX-2, TNF-α, IL-1β and IL-6. Hydrophobic interactions between ligand **11e** and the active residues (with residues Pro131, Glu25, Tyr24, Ser84, Glu83, Leu82, Gln81, Leu80, Phe133, Val132) of the IL-1β protein are showed in Table 3. The ligand docked with the IL-1β protein showed a −9.3 kcal/mol binding energy. The binding profile of compound **11e** docked with TNF-α showed a −8.6 kcal/mol binding energy. The hydrophobic interactions between the compound **11e** and the active residues of the TNF-α protein were Phe144, Ala145, Glu146, Ser147, Val150, Gly148, Val17, Arg32, Ala18 and Pro20. The pose of the docked ligand–protein IL-6 interaction was found to have a −8.1 kcal/mol binding energy. The hydrophobic interactions between the ligand and the active residues of the protein were Lys27, Tyr31, Gln111, Gly35, Glu110, Ala114, Ser118, Val121 and Gln28. The docking and binding affinity of compound **11a** for the IL-6 active site exhibited one hydrogen bond between its C═O group and the NH_2 of Arg30.The docking and binding affinity of compound **11i** for COX-2 and the TNF-α active site exhibited one or three hydrogen bonds between its C═O group and the NH_2 of Gln289, Phe144, Ala145 and Gln67, respectively.

Studies on the docking of compound **11e** to pro-inflammatory cytokines revealed the alteration and function of compound **11e** on its corresponding target proteins. The acquired structure–activity relationship shows that appropriately substituted derivatives have the necessary geometry to provide potent and selective inhibition of the iNOS and COX-2 receptors and exhibit excellent anti-inflammatory activities. It is worth mentioning that compound **11e** may exert significant anti-inflammatory activities by inhibiting the target proteins iNOS and COX-2. The regulation of these cytokines was confirmed in *in vitro* studies examining the immunomodulation potential of compound **11e**.

4. Conclusion

In conclusion, we efficiently synthesized a series of novel steroidal chalcones with 3β-pregnenolone esters of cinnamic acid derivatives **11a-11i**. Among the tested compounds, 3β-3-phenyl acrylate-pregn-5-en-17β-yl-3′ -(p-fluoro)-phenylprop-2′-en-1′-one (**11e**) showed potent inhibition of inflammatory enzymes. Compound **11e** bearing chalcone analogues (1, 3-diphenyl-2-propen-1-one) and styryl ketone (*trans*-4-phenyl-3-buten-2-one) pharmacophores in the side chain plays a vital role in determining the preferences for the target sites. The significant inhibitory action of compound **11e** could be due to the presence of aryl groups with strong electron withdrawing substituents such as fluorine.

Later, the potent NO inhibitor **11e** was screened for its anti-inflammatory activity against RAW 264.7 cells. We found that compound **11e** exhibited the most potent activity for the inhibition of NO production, with an IC_{50} value of 1.46 μM, in LPS-induced RAW 264.7 cells. We also showed that compound **11e** exhibited promising inhibitory effects on the expression of pro-inflammatory factors, including TNF-α, IL-6, and PGE-2, *in vitro*. Compound **11e** significantly inhibited the LPS-induced expression of iNOS, TNF-α, IL-6, and COX-2 mRNA in a dose-dependent manner in RAW 264.7 cells. Furthermore, the anti-inflammatory effects of compound **11e** were likely achieved through the inhibition of NF-κB signal transduction pathways in activated RAW 264.7 cells. The molecular binding of compound **11e** to pro-inflammatory and anti-inflammatory cytokines asserted the alteration/function of the corresponding target proteins. The docked pose of compound **11e** with the target proteins (iNOS, COX-2, TNF-α, IL-1β, and IL-6) confirmed that compound **11e** acted as an anti-inflammatory mediator. Collectively, our initial pharmacological data revealed that these novel structural compounds, especially compound **11e,** might serve as useful lead compounds for the development of therapeutic agents for inflammation-related diseases.

Acknowledgements

This work was supported by a grant from Guangdong province Special Funds for Science and Technology of China (Shantou Government No. [2019] 113-66), and the teamwork projects were funded by Guangdong collaborative innovation and environment construction Foundation of China (No. 2016B090918129) and Shantou Science and Technology Project (No. [2019] 77-5) and Shantou Science and Technology Project (No. [2018] 155-11).

Author Contributions

Xiaorui Cai and Yicun Chen designed the research; Xiaorui Cai performed the synthetic work, Yicun Chen was responsible for the direction of the biological research, Xiaorui Cai, Fei Sha and Chuanyi Zhao performed the anti-inflammatory activity. Xiaorui Cai wrote the manuscript, and Yicun Chen was responsible for the correspondence of the manuscript. All authors discussed, edited and approved the final version.

Conflicts of Interest

The authors declare no conflict of interest.

References

[1] S.E. Byeon, J.Y. Chung, Y.G. Lee, B.H. Kim, K.H. Kim, J.Y. Cho, *In vitro* and *in vivo* anti-inflammatory effects of taheebo, a water extract from the inner bark of

Tabebuia avellanedae, Journal of Ethnopharmacology 119 (1) (2008) 145–152, https://doi.org/10.1016/j.jep.2008.06.016.
[2] X. Niu, H. Zhang, W. Li, Q. Mu, H. Yao, Y.u. Wang, Anti-inflammatory Effects of Cavidine *In Vitro* and *In Vivo*, a Selective COX-2 Inhibitor in LPS-Induced Peritoneal Macrophages of Mouse, Inflammation 38 (2) (2015) 923–933, https://doi.org/10.1007/s10753-014-0054-4.
[3] W. Li, H. Huang, Y. Zhang, T. Fan, X. Liu, W. Xing, X. Niu, Anti-inflammatory effect of tetrahydrocoptisine from *Corydalis impatiens* is a function of possible inhibition of TNF-α, IL-6 and NO production in lipopolysaccharide-stimulated peritoneal macrophages through inhibiting NF-κB activation and MAPK pathway, European Journal of Pharmacology 715 (1-3) (2013) 62–71, https://doi.org/10.1016/j.ejphar.2013.06.017.
[4] Y. Zhang, C. Liu, B. Dong, X. Ma, L. Hou, X. Cao, C. Wang, Anti-inflammatory Activity and Mechanism of Surfactin in Lipopolysaccharide-Activated Macrophages, Inflammation 38 (2) (2015) 756–764, https://doi.org/10.1007/s10753-014-9986-y.
[5] O. Hennebert, M.-A. Pelissier, S. Le Mee, E. Wülfert, R. Morfin, Anti-inflammatory effects and changes in prostaglandin patterns induced by 7β-hydroxy-epiandrosterone in rats with colitis, The Journal of Steroid Biochemistry and Molecular Biology 110 (3-5) (2008) 255–262, https://doi.org/10.1016/j.jsbmb.2007.12.014.
[6] A.S. Andreasen, K.S. Krabbe, R. Krogh-Madsen, S. Taudorf, B.K. Pedersen, K. Møller, Human endotoxemia as a model of systemic inflammation, Curr. Med. Chem. 15 (2008) 1697–1705.
[7] X. Zhu, Y. Liu, S. Liu, F. Diao, R. Xu, X. Ni, Lipopolysaccharide primes macrophages to increase nitric oxide production in response to *Staphylococcus Aureus*, Immunology Letters 112 (2) (2007) 75–81, https://doi.org/10.1016/j.imlet.2007.06.007.
[8] R.M. Mohareb, G.A. Elmegeed, O.M.E. Abdel-Salam, S.H. Doss, M.G. William, Synthesis of modified steroids as a novel class of non-ulcerogenic, anti-inflammatory and anti-nociceptive agents, Steroids 76 (10-11) (2011) 1190–1203, https://doi.org/10.1016/j.steroids.2011.05.011.
[9] S. Sadeghi, C.J. Bain, N. Pandeya, P.M. Webb, A.C. Green, D.C. Whiteman, Aspirin, Nonsteroidal Anti-inflammatory Drugs, and the Risks of Cancers of the Esophagus, Cancer Epidemiol Biomarkers Prev 17 (5) (2008) 1169–1178, https://doi.org/10.1158/1055-9965.EPI-07-2852.
[10] T. Shimada, M. Matsumoto, Y. Tatsumi, A. Kanamaru, S. Akira, A novel lipopolysaccharide inducible C-C chemokine receptor related gene in murine macrophages, FEBS Lett. 425 (1998) 490–494.
[11] H. Li, J.-H. Yoon, H.-J. Won, H.-S. Ji, H.J. Yuk, K.H. Park, H.-Y. Park, T.-S. Jeong, Isotrifoliol inhibits pro-inflammatory mediators by suppression of TLR/NF-κB and TLR/MAPK signaling in LPS-induced RAW264.7 cells, International Immunopharmacology 45 (2017) 110–119, https://doi.org/10.1016/j.intimp.2017.01.033.
[12] T. Collins, M.I. Cybulsky, NF-κB: pivotal mediator or innocent bystander in atherogenesis? J. Clin. Invest. 107 (3) (2001) 255–264, https://doi.org/10.1172/JCI10373.
[13] T. Kawai, S. Akira, The role of pattern-recognition receptors in innate immunity: update on Toll-like receptors, Nat. Immunol. 11 (2010) 373–384.
[14] K.K. Sanjeewa, I.P. Fernando, E.A. Kim, G. Ahn, Y. Jee, Y.J. Jeon, Anti-inflammatory activity of a sulfated polysaccharide isolated from an enzymatic digest of brown seaweed Sargassum horneri in RAW 264.7 cells, Nutr. Res. Pract. 11 (2017) 3–10.
[15] T. Lou, W. Jiang, D. Xu, T. Chen, Y. Fu, Inhibitory Effects of Polydatin on Lipopolysaccharide-Stimulated RAW 264.7 Cells, Inflammation 38 (3) (2015) 1213–1220, https://doi.org/10.1007/s10753-014-0087-8.
[16] X. Ci, R. Ren, K. Xu, H. Li, Q. Yu, Y.u. Song, D. Wang, R. Li, X. Deng, Schisantherin A Exhibits Anti-inflammatory Properties by Down-Regulating NF-κB and MAPK Signaling Pathways in Lipopolysaccharide-Treated RAW 264.7 Cells, Inflammation 33 (2) (2010) 126–136, https://doi.org/10.1007/s10753-009-9166-7.
[17] M.J. Sung, M. Davaatseren, W. Kim, S.K. Park, S.H. Kim, H.J. Hur, M.S. Kim, Y. S. Kim, D.Y. Kwon, Vitisin A suppresses LPS-induced NO production by inhibiting ERK, p38, and NF-κB activation in RAW 264.7 cells, Int. Immunopharmacol 9 (2009) 319–323.
[18] Y. Huang, J. Cui, S. Chen, C. Gan, A. Zhou, Synthesis and antiproliferative activity of some steroidal lactams, Steroids 76 (12) (2011) 1346–1350, https://doi.org/10.1016/j.steroids.2011.06.013.
[19] G.-W. Fan, X.-M. Gao, H. Wang, Y. Zhu, J.u. Zhang, L.-M. Hu, Y.-F. Su, L.-Y. Kang, B.-L. Zhang, The anti-inflammatory activities of Tanshinone IIA, an active component of TCM, are mediated by estrogen receptor activation and inhibition of iNOS, The Journal of Steroid Biochemistry and Molecular Biology 113 (3-5) (2009) 275–280, https://doi.org/10.1016/j.jsbmb.2009.01.011.
[20] M. Singh, A.A. Hamid, A.K. Maurya, O.m. Prakash, F. Khan, A. Kumar, O. O. Aiyelaagbe, A.S. Negi, D.U. Bawankule, Synthesis of diosgenin analogues as potential anti-inflammatory agents, The Journal of Steroid Biochemistry and Molecular Biology 143 (2014) 323–333, https://doi.org/10.1016/j.jsbmb.2014.04.006.
[21] N.-J. Fan, J.-J. Tang, H.e. Li, X.-J. Li, B.o. Luo, J.-M. Gao, Synthesis and cytotoxic activity of some novel steroidal C-17 pyrazolinyl derivatives, European Journal of Medicinal Chemistry 69 (2013) 182–190, https://doi.org/10.1016/j.ejmech.2013.08.016.
[22] X.G. Bai, C.L. Xu, S.S. Zhao, H.W. He, Y.C. Wang, J.X. Wang, Synthesis and cytotoxic evaluation of alkoxylated chalcones, Molecules. 19 (2014) 17256–17278.
[23] B.P. Bandgar, S.S. Gawande, R.G. Bodade, J.V. Totre, C.N. Khobragade, Synthesis and biological evaluation of simple methoxylated chalcones as anticancer, anti-inflammatory and antioxidant agents, Bioorganic & Medicinal Chemistry 18 (3) (2010) 1364–1370, https://doi.org/10.1016/j.bmc.2009.11.066.
[24] H.N. ElSohly, A.S. Joshi, A.C. Nimrod, L.A. Walker, A.M. Clark, Antifungal chalcones from Maclura tinctoria, Planta Med.67 (2001) 87–89.
[25] D. Kakati, R.K. Sarma, R. Saikia, N.C. Barua, J.C. Sarma, Rapid microwave assisted synthesis and antimicrobial bioevaluation of novel steroidal chalcones, Steroids 78 (3) (2013) 321–326, https://doi.org/10.1016/j.steroids.2012.12.003.
[26] B.A. Bhat, K.L. Dhar, S.C. Puri, A.K. Saxena, M. Shanmugavel, G.N. Qazi, Synthesis and biological evaluation of chalcones and their derived pyrazoles as potential cytotoxic agents, Bioorganic & Medicinal Chemistry Letters 15 (12) (2005) 3177–3180, https://doi.org/10.1016/j.bmcl.2005.03.121.
[27] E.-E. Baulieu, P. Robel, Neurosteroids: A new brain function? The Journal of Steroid Biochemistry and Molecular Biology 37 (3) (1990) 395–403, https://doi.org/10.1016/0960-0760(90)90490-C.
[28] M. Iqbal Choudhary, M. Shahab Alam, Atta-ur-Rahman, S. Yousuf, Y.-C. Wu, A.-S. Lin, F. Shaheen, Pregnenolone derivatives as potential anticancer agents, Steroids 76 (14) (2011) 1554–1559, https://doi.org/10.1016/j.steroids.2011.09.006.
[29] Z. Yuan, J.P. Zhang, C. Yang, Ligusticum wallichii extract inhibited the expression of IL-1β after AMI in rats, Evid-Based Complement Alternat. Med. (2014) 1–8.
[30] F. Song, H. Li, J. Sun, S. Wang, Protective effects of cinnamic acid and cinnamic aldehyde on isoproterenol-induced acute myocardial ischemia in rats, Journal of Ethnopharmacology 150 (1) (2013) 125–130, https://doi.org/10.1016/j.jep.2013.08.019.
[31] J.C. Liao, J.S. Deng, C.S. Chiu, W.C. Hou, S.S. Huang, P.H. Shie, G.J. Huang, Anti-inflammatory activities of Cinnamomum cassia constituents in vitro and in vivo, Evid-Based Complement Alternat. Med. (2012) 1–12.
[32] O.M. Abd El-Raouf, E.M. El-Sayed, M.F. Manie, Cinnamic acid and cinnamaldehyde ameliorate cisplatin-induced splenotoxicity in rats, J. Biochem. Mol. Toxicol.29 (2015) 426–431.
[33] A. Magyar, J. Wölfling, M. Kubas, J.A. Cuesta Seijo, M. Sevvana, R. Herbst-Irmer, P. Forgó, G. Schneider, Synthesis of novel steroid-tetrahydroquinoline hybrid molecules and d-homosteroids by intramolecular cyclization reactions, Steroids 69 (5) (2004) 301–312, https://doi.org/10.1016/j.steroids.2004.01.004.
[34] G. Mehta, V. Singh, Hybrid systems through natural product leads: an approach towards new molecular entities, Chem. Soc. Rev. 31 (2002) 324–334.
[35] I.H. Lone, K.Z. Khan, B.I. Fozdar, F. Hussain, Synthesis antimicrobial and antioxidant studies of new oximes of steroidal chalcones, Steroids 78 (9) (2013) 945–950, https://doi.org/10.1016/j.steroids.2013.05.015.
[36] R. Hirschmann, N.G. Steinberg, P. Buchschacher, J.H. Fried, G.J. Kent, M. Tishler, S.L. Steelman, Synthesis and structure of steroidal 4-pregneno [3, 2-c] pyrazoles: a novel class of potent anti-inflammatory steroids, J. Am. Chem. Soc. 85 (1963) 120–122.
[37] H.O. Saxena, U. Faridi, J.K. Kumar, S. Luqman, M.P. Darokar, K. Shanker, C.S. Chanotiya, M.M. Gupta, A.S. Negi, Synthesis of chalcone derivatives on steroidal framework and their anticancer activities, Steroids. 72 (2007) 892–900.
[38] B.S. Sisodia, A.S. Negi, M.P. Darokar, U.N. Dwivedi, S.P.S. Khanuja, Antiplasmodial activity of steroidal chalcones: evaluation of their effect on hemozoin synthesis and the new permeation pathway of *Plasmodium falciparum*-infected erythrocyte membrane, Chem. Biol. Drug. Des. 79 (2012) 610–615.
[39] A.H. Banday, B.P. Mir, I.H. Lone, K.A. Suri, H.M.S. Kumar, Studies on novel D-ring substituted steroidal pyrazolines as potential anticancer agents, Steroids 75 (12) (2010) 805–809, https://doi.org/10.1016/j.steroids.2010.02.014.
[40] H. Wang, J.H. Zheng, W.J. Xu, C. Chen, D.C. Wei, W.X. Ni, Y. Pan, A new series of cytotoxic pyrazoline derivatives as potential anticancer agents that induce cell cycle arrest and apoptosis, Molecules. 22 (2017)1635-1648.
[41] X.K. Liu, B.J. Ye, Y. Wu, J.X. Nan, Z.H. Lin, H.R. Piao, Synthesis and antitumor activity of dehydroepiandrosterone derivatives on Es-2, A549, and HepG2 cells in vitro, Chem. Biol. Drug. Des. 79 (2012) 523–529.
[42] X. Cai, S. Zhao, D.e. Cai, J. Zheng, Z. Zhu, D. Wei, Z. Zheng, H. Zhu, Y. Chen, Synthesis and evaluation of novel D-ring substituted steroidal pyrazolines as potential anti-inflammatory agents, Steroids 146 (2019) 70–78, https://doi.org/10.1016/j.steroids.2019.03.012.
[43] O. Trott, A.J. Olson, AutoDock Vina: improving the speed and accuracy of docking with a new scoring function, efficient optimization and multithreading, J. Comput. Chem. 31 (2010) 455–461.
[44] H. Sun, W. Cai, X.u. Wang, Y. Liu, B. Hou, X. Zhu, L. Qiu, Vaccaria hypaphorine alleviates lipopolysaccharide-induced inflammation via inactivation of NFκB and ERK pathways in Raw 264.7 cells, BMC Complement Altern Med 17 (1) (2017), https://doi.org/10.1186/s12906-017-1635-1.
[45] A. Baskaran, K.K. Chua, V. Sabaratnam, M.R. Ram, U.R. Kuppusamy, *Pleurotus giganteus* (Berk. Karun & Hyde), the giant oyster mushroom inhibits NO production in LPS/$_{H}$2$_{O}$2 stimulated RAW 264.7 cells via STAT 3 and COX-2 pathways, BMC Complem Altern M. 17 (2017) 40–48.

[46] R. Anand, G. Kaithwas, Anti-inflammatory potential of alpha-linolenic acid mediated through selective COX inhibition: computational and experimental data, Inflammation. 37 (2014) 1297–1306.

[47] S. Saravanan, P. Pandikumar, N.P. Babu, V.I.H. Islam, K. Thirugnanasambantham, M.G. Paulraj, K. Balakrishna, S. Ignacimuthu, *In Vivo* and *In Vitro* Immunomodulatory Potential of Swertiamarin Isolated from *Enicostema axillare* (Lam.) A. Raynal That Acts as an Anti-inflammatory Agent, Inflammation 37 (5) (2014) 1374–1388, https://doi.org/10.1007/s10753-014-9862-9.

[48] X. Fang, Y. Yin, Y.T. Chen, L. Yao, B.o. Wang, M.D. Cameron, L.i. Lin, S. Khan, C. Ruiz, T. Schröter, W. Grant, A. Weiser, J. Pocas, A. Pachori, S. Schürer, P. LoGrasso, Y. Feng, Tetrahydroisoquinoline Derivatives As Highly Selective and Potent Rho Kinase Inhibitors, J. Med. Chem. 53 (15) (2010) 5727–5737, https://doi.org/10.1021/jm100579r.

[49] A. Sun, J.-J. Yoon, Y. Yin, A. Prussia, Y. Yang, J. Min, R.K. Plemper, J.P. Snyder, Potent Non-Nucleoside Inhibitors of the Measles Virus RNA-Dependent RNA Polymerase Complex, J. Med. Chem. 51 (13) (2008) 3731–3741, https://doi.org/10.1021/jm701239a.